Joint Transceiver Design Algorithms for Multiuser MISO Relay Systems With Energy Harvesting

Yunlong Cai, *Senior Member, IEEE*, Ming-Min Zhao, Qingjiang Shi, Benoit Champagne, *Senior Member, IEEE*, and Min-Jian Zhao, *Member, IEEE*

***Abstract*— In this paper, we investigate a multiuser multiple-input single-output relay system with simultaneous wireless information and power transfer, where the received signal is divided into two parts for information decoding and energy harvesting (EH), respectively. Assuming that both base station (BS) and relay station (RS) are equipped with multiple antennas, we study the joint transceiver design problem for the BS beamforming vectors, the RS amplify-and-forward transformation matrix, and the power splitting (PS) ratios at the single-antenna receivers. The aim is to minimize the total transmission power of the BS and the RS under both signal-to-interference-plus-noise ratio and EH constraints. First, an iterative algorithm based on alternating optimization (AO) and with guaranteed convergence is proposed to successively optimize the transceiver coefficients. This AO-based approach is then extended into a robust transceiver design against norm bounded errors in channel state information (CSI), by using semidefinite relaxation and the S-procedure. Second, a novel design scheme based on switched relaying (SR) is proposed that can significantly reduce the computational complexity and overhead of the AO-based designs while maintaining a similar performance. In the proposed SR scheme, the RS is equipped with a codebook of permutation matrices. For each permutation matrix, a latent transceiver is designed, which consists of BS beamforming vectors, optimally scaled RS permutation matrix, and receiver PS ratios. For the given CSI, the optimal latent transceiver with the lowest total power consumption is selected for transmission. We propose concave–convex procedure-based and subgradient-type iterative algorithms, respectively, to design the latent transceivers under perfect and imperfect CSI. Simulation results are presented to validate the effectiveness of all the proposed algorithms.**

Manuscript received January 27, 2016; revised May 24, 2016 and July 26, 2016; accepted August 29, 2016. Date of publication September 2, 2016; date of current version October 14, 2016. The work of Y. Cai, M. M. Zhao, and M. J. Zhao was supported in part by the National Natural Science Foundation of China under Grant 61471319, the Zhejiang Provincial Natural Science Foundation of China under Grant LY14F010013, the Scientific Research Project of Zhejiang Provincial Education Department under Grant Y201122655, and the Fundamental Research Funds for the Central Universities. The work of Q. Shi was supported by the National Nature Science Foundation of China under Grants 61671411 and 61302076. The associate editor coordinating the review of this paper and approving it for publication was S. Durrani.

Y. Cai, M.-M. Zhao, and M.-J. Zhao are with the College of Information Science and Electronic Engineering, Zhejiang University, Hangzhou 310027, China (e-mail: ylcai@zju.edu.cn; zmmblack@zju.edu.cn; mjzhao@zju.edu.cn).

Q. Shi is with the School of Information and Science Technology, Zhejiang Sci-Tech University, Hangzhou 310018, China (e-mail: qing.j.shi@gmail.com).

B. Champagne is with the Department of Electrical and Computer Engineering, McGill University, Montreal, QC H3A 0E9, Canada (e-mail: benoit.champagne@mcgill.ca).

Color versions of one or more of the figures in this paper are available online at http://ieeexplore.ieee.org.

Digital Object Identifier 10.1109/TCOMM.2016.2605688

***Index Terms*— Beamforming, concave-convex procedure, MISO relay, power splitting, energy harvesting, SWIPT.**

I. Introduction

RECENTLY, electromagnetic (EM) energy transfer techniques have attracted considerable interest in the wireless research community. Indeed, by exploiting the radiative far-field properties of EM waves, these techniques could in theory enable a radio receiver to harvest energy from its environment, thereby relaxing the battery requirements on user devices. An interesting application of wireless energy transfer is to jointly transmit information and energy using the same waveform, which is known as simultaneous wireless information and power transfer (SWIPT). The idea of SWIPT was first proposed by Varshney in [1], who characterizes the rate-energy (R-E) tradeoff in a discrete memoryless channel. The study of the R-E tradeoff was later extended to frequency selective fading channels in [2]. Popovski and Simeone [3] studied a two-way communication scenario with noiseless channels and limited resources, with emphasis on the tradeoffs due to the need of balancing the information flow with the resulting energy exchange among the communicating nodes. Fouladgar and Simeone [4] focused on multiuser systems and demonstrated that energy transfer constraints call for additional coordination among distributed nodes of a wireless network. However, the above schemes have not been fully realized yet due to practical circuit limitations.

A. Prior Work

The first practical receiver structure that makes SWIPT possible was proposed in [5], where two practical signal separation schemes were considered, namely, time switching (TS), where the receiver switches between information decoding (ID) and energy harvesting (EH), and power splitting (PS), where the received signal is split into two streams, such that a fraction ρ ($0 \leq \rho \leq 1$) of the received signal power is used for ID while the remaining fraction $(1-\rho)$ is used for EH. PS-based transceiver design algorithms were considered in [6]–[10]. Liu *et al.* [6] derived the optimal PS rule at the receiver, for both SISO (single-input single-output) and SIMO (single-input multiple-output) systems, in order to optimize the R-E performance tradeoff. Zhou *et al.* [7] proposed two practical receiver architectures, i.e., separated and integrated information and energy receivers, based on dynamic power splitting. These authors characterized the R-E performance by taking circuit power consumption into account.

Shi *et al.* [8] studied the joint beamforming and power splitting (JBPS) design for a multiuser multiple-input single-output (MISO) broadcast system with SWIPT. In this study, the total transmission power at the base station (BS) is minimized subject to signal-to-interference-plus-noise ratio (SINR) and EH constraints for all the receivers. The JBPS problem for a K-user MISO interference channel was considered in [9], where the authors used the semidefinite relaxation (SDR) technique to address the non-convex problem and proved that the SDR is tight in the case of $K = 2$ or 3. Different from the approach of [9], an alternative second-order-cone-programming (SOCP) relaxation method was proposed in [10]. The SOCP relaxation based method guarantees a feasible solution to the JBPS problem and has lower complexity than the SDR method, while achieving a performance extremely close to the minimum transmission power. A primal-decomposition based decentralized algorithm was also presented in this work.

Besides, the SWIPT technique for relay systems was considered in [11]–[14]. Specifically, the authors of [11] proposed a joint source and relay precoding design algorithm to achieve different tradeoffs between the energy transfer and the information rate. In [12], the relay beamforming design problem for the SWIPT scheme was considered in a non-regenerative two-way multi-antenna relay network, where a global optimal solution, a local optimal solution and a low-complexity suboptimal solution were proposed. The design of a high-rate beamformer that supports multiple communication pairs and intended for SWIPT in wireless relay networks was considered in [13]. In [14], a game-theoretical framework was developed to address the distributed power splitting problem for SWIPT in relay interference channels. The aforementioned works assume the availability of perfect channel state information (CSI), which may be impractical in realistic implementations of these systems.

B. Contributions

In this paper, we consider the use of PS-based receivers in a general multiuser MISO relay system, i.e., where a multi-antenna relay station (RS) is incorporated into the traditional MISO multiuser setup, as in [15]–[17]. We focus our study on the downlink transmission where: (1) the BS first transmits the signals intended for different receivers via beamforming to the RS; (2) the RS then processes the received signals through an amplify-and-forward (AF) transformation matrix and broadcasts it to all the receivers, and; (3) finally, each receiver employs the PS technique to decode information and harvest energy simultaneously. We present an optimization framework for the joint design of the BS beamforming vectors, the RS AF transformation matrix and the receiver PS ratios aiming to minimize the total power consumption under a set of minimum SINR and EH constraints at the receivers. In this work, we shall assume that the proposed joint design algorithms are implemented at the BS.[1]

[1]In practical systems, it is preferable to implement most of the signal processing operations at the BS rather than the RS, because the former can be equipped with more powerful hardware while the latter is expected to have a simpler structure and low energy consumption [18]–[20].

To this end, we first propose an iterative algorithm based on alternating optimization (AO) and with guaranteed convergence to successively optimize the transceiver coefficients, i.e., the BS beamformers, the AF transformation matrix and the receiver PS ratios. We show that each subproblem can be relaxed as a semidefinite programming (SDP) problem by applying the SDR technique [21]. This AO-based approach is then extended into a robust transceiver design against norm bounded errors (NBE) in CSI, by relying on the SDR technique and the S-procedure [22], [23]. While the performance of the AO-based designs is remarkable, we note that in this approach, the BS needs to compute and send the complete AF matrix to the RS before transmission, which entails higher design complexity and signaling requirements for the overhead. Secondly, inspired by [24], we hence propose a switched relaying (SR) approach for multiuser MISO relay systems with energy harvesting, in order to reduce the design and implementation costs. In this proposed SR scheme, we equip the RS with a selected codebook of permutation matrices. For each codebook entry, we can obtain a permuted channel matrix and therefore create a latent transceiver, which includes the BS beamforming vectors, an optimally scaled relaying permutation matrix and the receiver PS ratios. Among the set of latent transceivers so obtained for given CSI, the optimal one is chosen according to a suitable criterion for transmission.

Specifically, the SR-based algorithm constructs the RS AF transformation matrix within each latent transceiver by multiplying a permutation matrix from the codebook with a power scaling factor. Before data transmission, the BS sends the index of the permutation matrix, the RS power scaling factor, and the PS ratios corresponding to the optimal transceiver to the RS and the receivers through signaling channels. Compared to the AO-based algorithms, the SR approach reduces the number of optimization variables from the complete RS AF transformation matrix to a single power scaling factor, which in turn significantly reduces the computational complexity and signaling overhead. To design the latent transceivers, an iterative algorithm based on the concave-convex procedure (CCCP) [25], [26] is proposed that uses the estimated CSI and is guaranteed to converge to a local optimal point. We show that each subproblem in the iterative algorithm can be formulated as an SOCP problem. For the case of imperfect CSI, by taking the NBE model into account, we propose a robust subgradient algorithm which utilizes the side information provided by standard convex solvers. A simplified SR-based transceiver design algorithm is also proposed with much reduced computational complexity, while achieving a performance extremely close to the non-simplified scheme. Finally, two efficient codebook design approaches are developed.

Simulation results demonstrate that the proposed transceiver design algorithms are capable of providing robustness against the effects of norm-bounded CSI errors. In particular, the SR-based algorithms using a small codebook of permutation matrices can achieve almost the same performance as the AO-based algorithms but with reduced design/implementation complexity and signaling overhead.

To summarize, the contribution of this paper is twofold:

1) By applying the SDR technique and the S-procedure, AO-based algorithms for the joint transceiver design in multiuser MISO relay systems are proposed for both cases of perfect and imperfect CSI.[2] In the proposed algorithm, we transform the original highly non-convex problems into a sequence of SDP problems and we show that with proper initialization, the AO-based algorithms may serve as performance benchmarks.

2) Novel SR design algorithms are proposed for both perfect and imperfect CSI cases with much reduced design and implementation costs.[3] Furthermore, simplified versions of the SR-based algorithms are provided along with two codebook design approaches.

C. Structure and Notations

The reminder of this paper is organized as follows. Section II presents the multiuser MISO relay system model, the channel error model and the problem formulation. In Section III, the AO-based transceiver design algorithms for both perfect and imperfect CSI cases are developed. Section IV discusses the SR-based transceiver scheme, including the proposed latent transceiver design algorithms and the codebook design methods. A complexity analysis of the proposed algorithms along with a discussion of their initialization are provided in Section V. Finally, computer simulations are used in Section VI to validate the proposed algorithms, while conclusions are drawn in Section VII.

Notations: Scalars, vectors and matrices are respectively denoted by lower case, boldface lower case and boldface upper case letters. For a square matrix $\mathbf{A}$, $\mathrm{Tr}(\mathbf{A})$, $\mathrm{rank}(\mathbf{A})$, $\mathbf{A}^T$, $\mathrm{conj}(\mathbf{A})$ and $\mathbf{A}^H$ denote its trace, rank, transpose, conjugate, and conjugate transpose respectively, while $\mathbf{A} \succeq \mathbf{0}$ means that $\mathbf{A}$ is a positive semidefinite matrix. $E\{\cdot\}$ denotes the statistical expectation. $\Re\{\cdot\}$ denotes the real part of a variable. The operator $\mathrm{vec}(\cdot)$ stacks the elements of a matrix in one long column vector, $\mathrm{invp}(x)$ denotes the inverse of the positive portion, i.e., $\frac{1}{\max(x,0)}$. $\|\cdot\|$, $(\cdot)!$ and $|\cdot|$ denote the Euclidean norm of a complex vector, the factorial operator, and the absolute value of a complex scalar, respectively. $\mathbb{C}^{m\times n}$ ($\mathbb{R}^{m\times n}$) denotes the space of $m \times n$ complex (real) matrices, and $\mathbb{R}_+$ ($\mathbb{R}_-$) denotes the set of positive (negative) real numbers. Finally, the symbol $\otimes$ denotes the Kronecker product of two vectors/matrices.

II. System Model and Problem Formulation

A. Proposed System Model

In this work, we consider a multiuser MISO relay system which consists of one BS, one RS, and K mobile receivers indexed by $k \in \mathcal{K} \triangleq \{1, \ldots, K\}$. The number of antennas at the BS and the RS is denoted as N_t and N_r, respectively, while each receiver is equipped with a single antenna. We assume that $K \leq \min\{N_t, N_r\}$, which provides sufficient degrees of freedom for signal detection. We also assume that the classical two-hop AF relaying protocol [28] is employed, and that the direct links between the BS and the receivers are sufficiently weak and hence can be ignored. Different from the conventional multiuser MISO relay channels [17], we here consider PS-based receivers. The received signal at each receiver is split into two separate signal streams with different power levels: one is sent to the EH receiver and the other one is diverted to the ID receiver [5], as shown in Fig. 1. Under the above assumptions, the signals are transmitted in two phases as explained below.

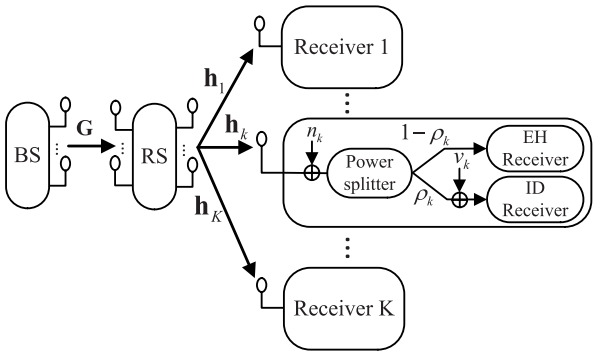

Fig. 1. The multiuser MISO relay system with PS-based receiver. Each receiver splits the received signal into two parts for ID and EH, respectively.

In the first phase, the BS transmits K data streams, each carrying an independent message intended for one of the K receivers. Thus, the transmitted data vector at the BS can be expressed as

$$\mathbf{x}_B = \sum_{k=1}^{K} \mathbf{f}_k s_k, \tag{1}$$

where s_k is the data signal for receiver k, with zero mean and variance $E\{|s_k|^2\} = 1$, and $\mathbf{f}_k \in \mathbb{C}^{N_t \times 1}$ denotes the transmit beamforming vector. The data signals $\{s_k\}_{k\in\mathcal{K}}$ are assumed to be statistically independent of each other. The transmit power of the BS can be shown as

$$P_B = E\{\mathbf{x}_B^H \mathbf{x}_B\} = \sum_{k=1}^{K} \|\mathbf{f}_k\|^2. \tag{2}$$

The transmission from the BS to the RS can be modeled as a standard point-to-point MIMO channel. Hence, the received data vector at the RS can be expressed as

$$\mathbf{y}_R = \mathbf{G} \sum_{k=1}^{K} \mathbf{f}_k s_k + \mathbf{n}_r, \tag{3}$$

where $\mathbf{G} \in \mathbb{C}^{N_r \times N_t}$ denotes the MIMO channel from the BS to the RS, and $\mathbf{n}_r \in \mathbb{C}^{N_r \times 1}$ is the complex circular Gaussian noise vector at the RS, with zero mean and covariance $E\{\mathbf{n}_r \mathbf{n}_r^H\} = \sigma_r^2 \mathbf{I}$, where σ_r^2 is the average noise power. It is assumed that

[2]Note that some of the mathematical constituent (the SDR technique and the S-procedure) used in this paper may coincide with our previous work [27] when considered in isolation, however the problems investigated in this work are totally different from that of [27] since the optimization of the RS AF transformation matrix is considered. Technically speaking, the problem considered in this work is more challenging since the variables are all coupled together including the RS AF transformation matrix.

[3] Unlike [24] where the mean squared error based precoder design problem is considered, we here focus on joint tranceiver design with SWIPT and aim to minimize the total transmission power of the BS and RS under both SINR and EH constraints. These two problems are quite different from a mathematical perspective and the proposed algorithms from [24] are not applicable here.

the transmitted signals $\{s_k\}_{k\in\mathcal{K}}$ are independent of the noise vector $\mathbf{n}_r$.

In the second phase, the RS forwards the received signal to all the receivers after performing a linear AF processing. Hence the vector signal transmitted from the RS can be formulated as

$$\mathbf{x}_R = \mathbf{W}\mathbf{y}_R, \tag{4}$$

where $\mathbf{W} \in \mathbb{C}^{N_r \times N_r}$ is the AF transformation matrix at the RS. The transmission power of the RS can be shown as

$$P_R = E\{\mathbf{x}_R\mathbf{x}_R^H\} = \sum_{k=1}^{K} \|\mathbf{W}\mathbf{G}\mathbf{f}_k\|^2 + \sigma_r^2\|\mathbf{W}\|^2. \tag{5}$$

Finally, The signal received at the kth receiver, $k \in \mathcal{K}$, is given by

$$y_k = \mathbf{h}_k^H\mathbf{x}_R + n_k = \mathbf{h}_k^H\mathbf{W}\mathbf{G}\sum_{k=1}^{K}\mathbf{f}_k s_k + \mathbf{h}_k^H\mathbf{W}\mathbf{n}_r + n_k, \tag{6}$$

where $\mathbf{h}_k \in \mathbb{C}^{N_r\times 1}$ denotes the complex conjugate channel vector between the RS and receiver k, and n_k is the additive noise introduced by the antenna at receiver k, which is assumed to be a complex circular Gaussian random variable with zero mean and variance σ_k^2.

Let $\rho_k\ (0 \le \rho_k \le 1)$ denote the PS ratio for receiver k, which means that a portion ρ_k of the signal power is used for signal detection while the remaining portion $1-\rho_k$ is diverted to an energy harvester. Thus, on the one hand, the signal available for ID at receiver k can be expressed as

$$r_k^{\mathrm{ID}} = \sqrt{\rho_k}\Big(\mathbf{h}_k^H\mathbf{W}\mathbf{G}\sum_{k=1}^{K}\mathbf{f}_k s_k + \mathbf{h}_k^H\mathbf{W}\mathbf{n}_r + n_k\Big) + \upsilon_k, \tag{7}$$

where υ_k is the additional complex circular Gaussian circuit noise with zero mean and variance $E\{|\upsilon_k|^2\} = \omega_k^2$, resulting from phase offsets and non-linearities during baseband conversion [5]. Consequently, the SINR at the kth receiver can be expressed as

$$\Gamma_k = \frac{\rho_k|\mathbf{h}_k^H\mathbf{W}\mathbf{G}\mathbf{f}_k|^2}{\rho_k\Big(\sum\limits_{j\neq k}^{K}|\mathbf{h}_k^H\mathbf{W}\mathbf{G}\mathbf{f}_j|^2 + \sigma_r^2\|\mathbf{h}_k^H\mathbf{W}\|^2 + \sigma_k^2\Big) + \omega_k^2}. \tag{8}$$

On the other hand, the total harvested energy that can be stored by receiver k is equal to

$$P_k^{\mathrm{EH}} = \xi_k(1-\rho_k)\Big(\sum_{j=1}^{K}|\mathbf{h}_k^H\mathbf{W}\mathbf{G}\mathbf{f}_j|^2 + \sigma_r^2\|\mathbf{h}_k^H\mathbf{W}\|^2 + \sigma_k^2\Big), \tag{9}$$

where $\xi_k \in (0, 1]$ denotes the energy conversion efficiency of the kth EH unit, which indicates that only a portion ξ_k of the radio frequency energy can be stored.

Remark 1: One potential application of the proposed system model is relay-assisted wireless sensor networks. With wireless power transfer, the sensor networks can scavenge energy from the surrounding radio environment, which guarantees a longer operating lifetime compared with conventional wireless sensor networks [29]. Furthermore, the deployment of relay nodes is an essential approach to provide ubiquitous high data rate and energy coverage.

B. Channel Error Model

We assume that the required CSI can be estimated at the BS and the RS by means of a suitable channel estimation algorithm [30]–[32]. In this work, we consider a time division duplex (TDD) mode and assume that the radio channels vary sufficiently slowly over time, so that the downlink transmit CSI can be obtained by channel reciprocity [33]. Also, since the BS and the RS are more powerful than the receivers, henceforth we assume that the BS can perfectly know the first phase CSI, i.e. $\mathbf{G}$, but not the second phase CSI, i.e. vectors $\{\mathbf{h}_k\}$. We employ the norm bounded error (NBE) model [34] to characterize the imperfections of the channel knowledge that may arise from, e.g., estimation errors, quantization effects, or combinations of both sources of errors [35], [36]. In particular, the true (but unknown) second phase CSI can be expressed as follows:

$$\mathbf{h}_k = \hat{\mathbf{h}}_k + \mathbf{e}_k, \quad k \in \mathcal{K}, \tag{10}$$

where $\hat{\mathbf{h}}_k$ denotes the estimated channel vector, while $\mathbf{e}_k$ denotes the CSI error vector. Note that in our considered channel model, $\hat{\mathbf{h}}_k$ is assumed to be available based on proper channel estimation methods, while the CSI error $\mathbf{e}_k$ is unknown. We also assume that $\mathbf{e}_k$ is bounded in its Euclidean norm, that is

$$\|\mathbf{e}_k\| \le \eta_k, \ \ k \in \mathcal{K}, \tag{11}$$

where η_k is a known positive constant. Equivalently, $\mathbf{h}_k$ belongs to the uncertainty set $\Re_k$ defined as

$$\Re_k = \{\mathbf{h}|\mathbf{h} = \hat{\mathbf{h}}_k + \mathbf{e}_k, \|\mathbf{e}_k\| \le \eta_k\}, \quad k \in \mathcal{K}. \tag{12}$$

The shape and the size of $\Re_k$ model the type of uncertainty in the estimated CSI, which is linked to the physical phenomenon producing the CSI errors. It should be emphasized that the actual errors $\mathbf{e}_k$ are assumed to be unknown while the corresponding upper bounds η_k can be obtained using preliminary knowledge about the main channel characteristics as wells as properties of the estimation and feedback mechanisms [35]. Note that an alternative channel error model is considered in [37], where the signal power is a function of the estimated CSI and there is an additive noise term that depends on the statistical estimation error characteristics.

C. Problem Formulation

In this subsection, we formulate the optimization problem for the joint design of $\mathbf{W}$, $\{\mathbf{f}_k\}_{k\in\mathcal{K}}$ and $\{\rho_k\}_{k\in\mathcal{K}}$ so as to minimize the total power consumption at the BS and the RS under the constraint that a set of minimum SINR and EH targets be satisfied at the receivers. In this study, we consider both perfect and imperfect CSI cases. The optimization problem

with perfect CSI can be expressed as[4]

$$\min_{\mathbf{W},\{\mathbf{f}_k,\,\rho_k\}} \quad P_B + P_R$$
$$\text{s.t. } \Gamma_k \geq \gamma_k,\ P_k^{\text{EH}} \geq \psi_k, \quad 0 \leq \rho_k \leq 1, \quad \forall k \in \mathcal{K}, \tag{13}$$

where in the evaluation of (8) and (9), the true channel vectors $\mathbf{h}_k$ are replaced by their estimates $\hat{\mathbf{h}}_k$.

Similarly, the robust optimization problem with imperfect CSI can be formulated as

$$\min_{\mathbf{W},\,\{\mathbf{f}_k,\,\rho_k\}} \quad P_B + P_R$$
$$\text{s.t. } \Gamma_k \geq \gamma_k, \quad P_k^{\text{EH}} \geq \psi_k, \quad \forall \|\mathbf{e}_k\|^2 \leq \eta_k^2,$$
$$0 \leq \rho_k \leq 1, \quad \forall k \in \mathcal{K}, \tag{14}$$

where in this case, the channel vectors in (8) and (9) are given by (10).

It is worth mentioning that, the received energy at each receiver should be above some threshold in order to activate the EH circuit [29]. This can be guaranteed by performing proper user scheduling, e.g., according to the distance between the RS and users. This paper focus on joint transceiver design with QoS guarantee for the scheduled users, as in most of the recent literature on EH related beamforming design, e.g. [9], [38], [39]. Note that problems (13) and (14) are in general non-convex, because both their objective functions and constraints are not convex in $\mathbf{W}$, $\{\mathbf{f}_k\}$ and $\{\rho_k\}$. Furthermore, (14) involves an infinite number of constraints. These characteristics make it intractable to obtain the global optimal solution for (13) and (14). In the sequel, we present two algorithms for obtaining suboptimal solutions to the above problems by applying proper convex optimization techniques, which are based on AO and SR, respectively.

III. Alternating Optimization Based Joint Transceiver Design

In this section, we present the AO-based transceiver design algorithms for the joint optimization of the BS beamforming vectors, the RS AF transformation matrix and the receiver PS ratios, for both perfect and imperfect CSI cases. In the proposed design, $\{\mathbf{f}_k, \rho_k\}_{k\in\mathcal{K}}$ and $\mathbf{W}$ are successively optimized in turn, while the other parameters are fixed. We show that each subproblem for the optimization of $\{\mathbf{f}_k, \rho_k\}$ or $\mathbf{W}$ can be reformulated as an SDP problem based on the SDR technique and the S-procedure. Furthermore, modified randomization techniques based on the worst-case concept are provided to recover a rank-one solution when higher-rank solutions are returned.

A. AO-Based Joint Transceiver Design With Perfect CSI

In the following, we introduce a joint transceiver design algorithm assuming perfect CSI. First, let us consider the optimization of $\{\mathbf{f}_k, \rho_k\}$ in (13) while the RS AF matrix $\mathbf{W}$ is fixed. The SDR technique can be applied to solve the remaining optimization problem by introducing a new variable $\mathbf{F}_k = \mathbf{f}_k\mathbf{f}_k^H$. Hence, problem (13) can be reformulated as follows by ignoring the rank-one constraints for all $\mathbf{F}_k$'s:

$$\min_{\{\mathbf{F}_k,\,\rho_k\}} \ \sum_{k=1}^{K}\text{Tr}(\mathbf{F}_k) + \sum_{k=1}^{K}\text{Tr}(\mathbf{Q}_k) + \sigma_r^2\|\mathbf{W}\|^2$$
$$\text{s.t. } \frac{1}{\gamma_k}\hat{\mathbf{h}}_k^H\mathbf{Q}_k\hat{\mathbf{h}}_k - \sum_{j\neq k}^{K}\hat{\mathbf{h}}_k^H\mathbf{Q}_j\hat{\mathbf{h}}_k \geq \sigma_r^2\|\hat{\mathbf{h}}_k^H\mathbf{W}\|^2 + \sigma_k^2 + \frac{\omega_k^2}{\rho_k},$$
$$\sum_{j=1}^{K}\hat{\mathbf{h}}_k^H\mathbf{Q}_j\hat{\mathbf{h}}_k \geq \frac{\psi_k}{\xi_k(1-\rho_k)} - \sigma_k^2 - \sigma_r^2\|\hat{\mathbf{h}}_k^H\mathbf{W}\|^2,$$
$$\mathbf{F}_k \succeq \mathbf{0}, \quad 0 \leq \rho_k \leq 1, \quad \forall k \in \mathcal{K}, \tag{15}$$

where $\mathbf{Q}_k = \mathbf{W}\mathbf{G}\mathbf{F}_k\mathbf{G}^H\mathbf{W}^H$. In this way, problem (13) is relaxed to a convex SDP problem, which can be efficiently solved by off-the-shelf algorithms [40]. Let $\{\mathbf{F}_k^*\}$ and $\{\rho_k^*\}$ denote the optimal solution to (15). Based on [8, Proposition 4.1], it can be verified that $\{\mathbf{F}_k^*\}$ and $\{\rho_k^*\}$ satisfy the first two sets of constraints of problem (15) with equality and $\{\mathbf{F}_k^*\}$ satisfy $\text{rank}(\mathbf{F}_k^*) = 1$, $\forall k$. Thus the optimal solution of problem (13) can be expressed as $\{\mathbf{f}_k^*, \rho_k^*\}$, where $\mathbf{f}_k^*$ is the principal component of $\mathbf{F}_k^*$, such that $\mathbf{F}_k^* = \mathbf{f}_k^*\mathbf{f}_k^{*H}$, $\|\mathbf{f}_k^*\| = \sqrt{f_k}$ and f_k is the largest eigenvalue of $\mathbf{F}_k^*$.

Next, we consider the optimization of the RS AF matrix $\mathbf{W}$ while assuming that $\{\mathbf{f}_k, \rho_k\}$ are fixed. Noting that $\mathbf{x}^T\mathbf{Y}\mathbf{z} = \text{vec}(\mathbf{x}\mathbf{z}^T)^T\text{vec}(\mathbf{Y})$, the numerator in (8) can be rewritten as

$$\rho_k|\hat{\mathbf{h}}_k^H\mathbf{W}\mathbf{G}\mathbf{f}_k|^2 = \rho_k|\mathbf{g}_{kk}^T\text{vec}(\mathbf{W})|^2 = \rho_k\mathbf{g}_{kk}^T\tilde{\mathbf{W}}\text{conj}(\mathbf{g}_{kk}), \tag{16}$$

where $\mathbf{g}_{kj} = \text{vec}(\text{conj}(\hat{\mathbf{h}}_k)\mathbf{f}_j^T\mathbf{G}^T)$ and $\tilde{\mathbf{W}} = \text{vec}(\mathbf{W})\text{vec}(\mathbf{W})^H$. Similarly, the denominator in (8) can be reformulated as

$$\rho_k\sum_{j\neq k}^{K}\mathbf{g}_{kj}^T\tilde{\mathbf{W}}\text{conj}(\mathbf{g}_{kj}) + \rho_k\sigma_r^2\sum_{j=1}^{N_r}\hat{\mathbf{h}}_k^H\mathbf{E}_j\tilde{\mathbf{W}}\mathbf{E}_j^H\hat{\mathbf{h}}_k + \rho_k\sigma_k^2 + \omega_k^2, \tag{17}$$

where $\mathbf{E}_k \in \{0,1\}^{N_r\times N_r^2}$ is a linear mapping matrix such that $\hat{\mathbf{h}}_k^H\mathbf{E}_j\text{vec}(\mathbf{W}) = \hat{\mathbf{h}}_k^H\mathbf{W}(:,j)$, where $\mathbf{W}(:,j)$ denotes the jth column of $\mathbf{W}$. With the help of (17) and (16), the SINR and EH constraints in problem (13) can be expressed as the following two inequalities:

$$\frac{1}{\gamma_k}\mathbf{g}_{kk}^T\tilde{\mathbf{W}}\text{conj}(\mathbf{g}_{kk}) - \sum_{j\neq k}^{K}\mathbf{g}_{kj}^T\tilde{\mathbf{W}}\text{conj}(\mathbf{g}_{kj})$$
$$-\sigma_r^2\sum_{j=1}^{N_r}\hat{\mathbf{h}}_k^H\mathbf{E}_j\tilde{\mathbf{W}}\mathbf{E}_j^H\hat{\mathbf{h}}_k \geq \sigma_k^2 + \frac{\omega_k^2}{\rho_k}, \tag{18}$$

$$\sum_{j=1}^{K}\mathbf{g}_{kj}^T\tilde{\mathbf{W}}\text{conj}(\mathbf{g}_{kj}) + \sigma_r^2\sum_{j=1}^{N_r}\hat{\mathbf{h}}_k^H\mathbf{E}_j\tilde{\mathbf{W}}\mathbf{E}_j^H\hat{\mathbf{h}}_k^H$$
$$\geq \frac{\psi_k}{\xi_k(1-\rho_k)} - \sigma_k^2. \tag{19}$$

[4]There is in practice a power consumption tradeoff between the BS and the RS [17], and a more general objective function could be $P_B + \alpha P_R$ where α is a positive weight. We assume that $\alpha = 1$ in this work, since this does not change the nature of the problem and its solution.

TABLE I
AO Perfect CSI : AO-BASED TRANSCEIVER DESIGN ALGORITHM WITH PERFECT CSI

1. Initialize $\mathbf{W}$ and define the tolerance of accuracy $\delta > 0$.
2. **Repeat**
   2.1 Solve problem (15) with fixed $\mathbf{W}$ to obtain the updated $\{\mathbf{f}_k, \rho_k\}$.
   2.2 Solve problem (20) with fixed $\{\mathbf{f}_k, \rho_k\}$ to obtain the updated $\mathbf{W}$. Employ the proposed rank-one recovery method in Appendix A if a higher-rank solution is returned when solving problem (20).
3. **Until** the total power consumption between two adjacent iterations is less than δ or the total power consumption of Step 2.2 is higher than that of Step 2.1.

Hence, (13) can be reformulated as the following SDP problem by employing the SDR technique:

$$\min_{\tilde{\mathbf{W}}} \sum_{k=1}^{K} \left(\|\mathbf{f}_k\|^2 + \mathrm{Tr}(\mathbf{C}_k \tilde{\mathbf{W}} \mathbf{C}_k^H) \right) + \sigma_r^2 \mathrm{Tr}(\tilde{\mathbf{W}})$$
$$\text{s.t. (18) and (19)}, \quad \tilde{\mathbf{W}} \succeq \mathbf{0}, \quad \forall k \in \mathcal{K}, \tag{20}$$

where $\mathbf{C}_k = (\mathbf{G}\mathbf{f}_k)^T \otimes \mathbf{I}_{N_r}$. Different from (15), the optimal solution $\tilde{\mathbf{W}}^*$ to problem (20) is not necessarily rank-one; hence a simple rank-one recovery method based on a randomization procedure but with lower complexity is proposed in Appendix A to address this issue.

The AO-based iterative algorithm to solve problem (13) is summarized in Table I. Regarding its convergence behavior, we have the following proposition.

Proposition 1: The proposed AO-based iterative algorithm in Table I is monotonic convergent.

Proof: Please refer to Appendix B. ∎

B. AO-Based Joint Transceiver Design With Imperfect CSI

In this subsection, we address the robust AO-based joint transceiver design for the case of imperfect CSI by employing the channel error model considered in Subsection II-B. We demonstrate that the corresponding subproblems can be converted to alternative forms where the concepts of SDR and S-procedure can be applied.

First, let us consider the optimization of $\{\mathbf{f}_k, \rho_k\}$ in (14) when $\mathbf{W}$ is fixed under imperfect CSI , i.e. $\mathbf{h}_k = \hat{\mathbf{h}}_k + \mathbf{e}_k$, $\forall k \in \mathcal{K}$. In this case, the SINR constraints in (15) can be replaced by the following quadratic form:

$$(\hat{\mathbf{h}}_k + \mathbf{e}_k)^H \mathbf{U}_k (\hat{\mathbf{h}}_k + \mathbf{e}_k) \geq \sigma_k^2 + \frac{\omega_k^2}{\rho_k}, \tag{21}$$

where $\mathbf{e}_k$ satisfy (11) and $\mathbf{U}_k$ can be expressed as

$$\mathbf{U}_k = \frac{1}{\gamma_k} \mathbf{Q}_k - \sum_{j \neq k}^{K} \mathbf{Q}_j - \sigma_r^2 \mathbf{W}\mathbf{W}^H. \tag{22}$$

Similarly, the EH constraints can be reformulated as the following expression:

$$(\hat{\mathbf{h}}_k + \mathbf{e}_k)^H \mathbf{V}_k (\hat{\mathbf{h}}_k + \mathbf{e}_k) + \sigma_k^2 \geq \frac{\psi_k}{\xi_k (1 - \rho_k)}, \quad \forall \|\mathbf{e}_k\|^2 \leq \eta_k^2, \tag{23}$$

where $\mathbf{V}_k = \sum_{j=1}^{K} \mathbf{Q}_j + \sigma_r^2 \mathbf{W}\mathbf{W}^H$.

By applying the S-procedure, the constraints in (21) and (23) can be reformulated as finite convex constraints, which are equivalent to the following two linear matrix inequality (LMI) constraints:

$$\begin{bmatrix} \mathbf{U}_k + \lambda_k \mathbf{I} & \mathbf{U}_k \hat{\mathbf{h}}_k \\ \hat{\mathbf{h}}_k^H \mathbf{U}_k & \hat{\mathbf{h}}_k^H \mathbf{U}_k \hat{\mathbf{h}}_k - \sigma_k^2 - \omega_k^2 p_k - \lambda_k \eta_k^2 \end{bmatrix} \succeq \mathbf{0}, \tag{24}$$

$$\begin{bmatrix} \mathbf{V}_k + \mu_k \mathbf{I} & \mathbf{V}_k \hat{\mathbf{h}}_k \\ \hat{\mathbf{h}}_k^H \mathbf{V}_k & \hat{\mathbf{h}}_k^H \mathbf{V}_k \hat{\mathbf{h}}_k + \sigma_k^2 - \frac{\psi_k}{\xi_k} q_k - \mu_k \eta_k^2 \end{bmatrix} \succeq \mathbf{0}, \tag{25}$$

where $p_k = \frac{1}{\rho_k}$, $q_k = \frac{1}{1-\rho_k}$, while $\lambda_k \geq 0$ and $\mu_k \geq 0$ are slack variables.

With (24) and (25), the robust counterpart of problem (15) can be reformulated as follows by ignoring the rank-one constraints for all $\mathbf{F}_k$'s:

$$\min_{\{\mathbf{F}_k,\, p_k,\, q_k,\, \lambda_k,\, \mu_k\}} \sum_{k=1}^{K} \mathrm{Tr}(\mathbf{F}_k) + \sum_{k=1}^{K} \mathrm{Tr}(\mathbf{Q}_k) + \sigma_r^2 \|\mathbf{W}\|^2$$
$$\text{s.t. (24) and (25)}, \lambda_k \geq 0, \ \mu_k \geq 0, \quad \mathbf{F}_k \succeq \mathbf{0},$$
$$p_k \geq 1, \quad q_k \geq 1, \quad \mathrm{invp}(p_k) + \mathrm{invp}(q_k) \leq 1, \quad \forall k \in \mathcal{K}, \tag{26}$$

where the last set of inequality constraints must be satisfied with equality at optimality, for otherwise, the objective value can be further decreased by decreasing p_k's. It is worth noting that different from problem (15) which always returns a rank-one solution, the optimal solution $\{\mathbf{F}_k^*\}$ of (26) may not be of rank-one, in which case, additional processing steps may be needed to extract a rank-one solution from the $\mathbf{F}_k^*$. To this end, a rank-one recovery method based on a randomization procedure is presented in Appendix A.

Next, we consider the optimization of the RS AF matrix $\mathbf{W}$ with fixed $\{\mathbf{f}_k, \rho_k\}$. Similar to Subsection III-A, we have the following expression:

$$\begin{aligned} \mathbf{g}_{kj} &= \mathrm{vec}(\mathrm{conj}(\mathbf{h}_k)\mathbf{f}_j^T \mathbf{G}^T) = (\mathbf{G}\mathbf{f}_j \otimes \mathbf{I}_{N_r})\mathrm{conj}(\mathbf{h}_k) \\ &= \hat{\mathbf{G}}_j \mathrm{conj}(\mathbf{h}_k), \end{aligned} \tag{27}$$

where $\hat{\mathbf{G}}_j = \mathbf{G}\mathbf{f}_j \otimes \mathbf{I}_{N_r}$, $j \in \mathcal{K}$. Thus, the robust version of (18) can be formulated as

$$\begin{aligned} &\frac{1}{\gamma_k} (\hat{\mathbf{h}}_k^H + \mathbf{e}_k^H) \overline{\mathbf{W}}_k (\hat{\mathbf{h}}_k + \mathbf{e}_k) - \sum_{j \neq k}^{K} (\hat{\mathbf{h}}_k^H + \mathbf{e}_k^H) \overline{\mathbf{W}}_j (\hat{\mathbf{h}}_k + \mathbf{e}_k) \\ &- \sigma_r^2 \sum_{j=1}^{N_r} (\hat{\mathbf{h}}_k^H + \mathbf{e}_k^H) \mathbf{E}_j \tilde{\mathbf{W}} \mathbf{E}_j^H (\hat{\mathbf{h}}_k + \mathbf{e}_k) \\ &\geq \sigma_k^2 + \frac{\omega_k^2}{\rho_k}, \quad \forall \|\mathbf{e}_k\|^2 \leq \eta_k^2, \quad k \in \mathcal{K}, \end{aligned} \tag{28}$$

where $\overline{\mathbf{W}}_j = \hat{\mathbf{G}}_j^T \tilde{\mathbf{W}} \mathrm{conj}(\hat{\mathbf{G}}_j)$, and $\tilde{\mathbf{W}}$ has already been defined in Subsection III-A. By applying the S-procedure, we can transform (28) into the following LMIs:

$$\begin{bmatrix} \tilde{\mathbf{U}}_k + \lambda_k \mathbf{I} & \tilde{\mathbf{U}}_k \hat{\mathbf{h}}_k \\ \hat{\mathbf{h}}_k^H \tilde{\mathbf{U}}_k & \hat{\mathbf{h}}_k^H \tilde{\mathbf{U}}_k \hat{\mathbf{h}}_k - \sigma_k^2 - \omega_k^2 p_k - \lambda_k \eta_k^2 \end{bmatrix} \succeq \mathbf{0}, \tag{29}$$

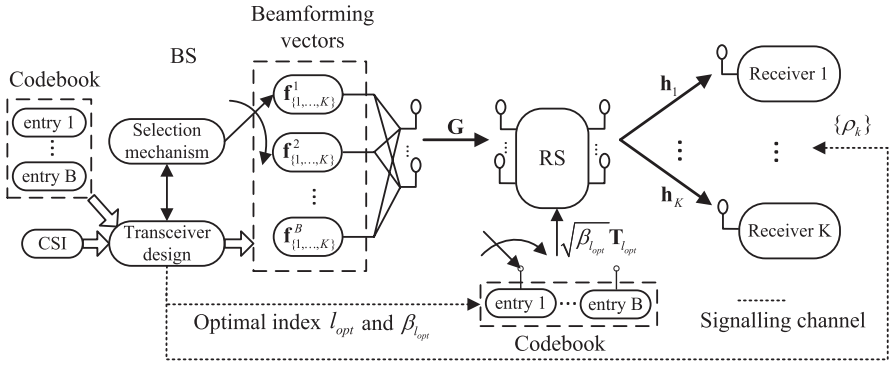

Fig. 2. Transceiver scheme with SR for multiuser MISO relay system (the dashed line denotes signaling channels).

TABLE II

AO Imperfect CSI : AO-BASED ROBUST TRANSCEIVER DESIGN ALGORITHM WITH IMPERFECT CSI

1. Initialize $\mathbf{W}$ and define the tolerance of accuracy $\delta > 0$.
2. **Repeat**
   - 2.1 Solve problem (26) with fixed $\mathbf{W}$ to obtain the updated $\{\mathbf{F}_k, \rho_k\}$. If $\{\mathbf{F}_k\}$ are rank-one matrices, use their principal eigenvectors to obtain the desired solutions $\{\mathbf{f}_k\}$, otherwise, employ the rank-one recovery method in Appendix A to recover rank-one solutions from $\{\mathbf{F}_k\}$.
   - 2.2 Solve problem (31) with fixed $\{\mathbf{F}_k, \rho_k\}$ to obtain the updated $\mathbf{W}$. If $\tilde{\mathbf{W}}$ is a rank-one matrix, use its principal eigenvector as a solution. Otherwise, employ the method in Appendix A to recover a rank-one solution from $\tilde{\mathbf{W}}$.
3. **Until** the total power consumption between two adjacent iterations is less than δ or increased.

where $\tilde{\mathbf{U}}_k = \frac{1}{\gamma_k}\overline{\mathbf{W}}_k - \sum_{j\neq k}^{K}\overline{\mathbf{W}}_j - \sigma_r^2\sum_{k=1}^{N_r}\mathbf{E}_k\tilde{\mathbf{W}}\mathbf{E}_k^H$ and $\lambda_k \geq 0$. Similarly, the robust version of (19) can be formulated as

$$\begin{bmatrix} \tilde{\mathbf{V}}_k + \mu_k\mathbf{I} & \tilde{\mathbf{V}}_k\hat{\mathbf{h}}_k \\ \hat{\mathbf{h}}_k^H\tilde{\mathbf{V}}_k & \hat{\mathbf{h}}_k^H\tilde{\mathbf{V}}_k\hat{\mathbf{h}}_k + \sigma_k^2 - \frac{\psi_k}{\xi_k}q_k - \mu_k\eta_k^2 \end{bmatrix} \succeq \mathbf{0}, \quad (30)$$

where $\tilde{\mathbf{V}}_k = \sum_{j=1}^{K}\overline{\mathbf{W}}_k + \sigma_r^2\sum_{k=1}^{N_r}\mathbf{E}_k\tilde{\mathbf{W}}\mathbf{E}_k^H$ and $\mu_k \geq 0$. Hence, problem (14) with fixed $\{\mathbf{f}_k, \rho_k\}$ can be formulated as the following SDP problem with the SDR technique:

$$\min_{\tilde{\mathbf{W}},\,\{\lambda_k,\,\mu_k\}} \sum_{k=1}^{K}\left(\|\mathbf{f}_k\|^2 + \mathrm{Tr}(\mathbf{C}_k\tilde{\mathbf{W}}\mathbf{C}_k^H)\right) + \sigma_r^2\mathrm{Tr}(\tilde{\mathbf{W}})$$
$$\text{s.t. (29) and (30)}, \quad \tilde{\mathbf{W}} \succeq \mathbf{0},\ \lambda_k \geq 0, \quad \mu_k \geq 0, \quad \forall k, \quad (31)$$

where $\mathbf{C}_k$ has been defined in Subsection III-A. Note that the optimal solution of (31) is also not necessarily rank-one and thus we can once again employ the method in Appendix A to address this issue.

We summarize the AO-based robust joint transceiver design algorithm in Table II. For practical implementation, the optimally designed AF matrix $\mathbf{W}$ and PS ratios $\{\rho_k\}$ should be fed forward through signaling channels from the BS to the RS and receivers, respectively, prior to data transmission. Similar to Proposition 1, the monotonic convergence of the proposed robust algorithm is guaranteed.

IV. SWITCHED RELAYING BASED JOINT TRANSCEIVER DESIGN

In the previous section, we proposed novel AO-based transceiver design algorithms. As will be shown in Section VI, these algorithms can achieve a good performance in transmission, but they are characterized by higher signaling overhead and computational complexity. In this section, motivated by these considerations, we develop alternative SR-based transceiver design algorithms that are more efficient and simpler to implement. As illustrated in Fig. 2, we equip the RS with a finite codebook of permutation matrices,[5] i.e., $\Upsilon = \{\mathbf{T}_1, \mathbf{T}_2, \ldots, \mathbf{T}_B\}$, where $\mathbf{T}_l \in \{0,1\}^{N_r\times N_r}$ is the l-th matrix in the codebook, index $l \in \{1, \ldots, B\}$ and B denotes the codebook size which satisfies $B \ll N_r!$.[6] In order to reduce the signaling overhead and the number of optimization variables, the RS AF matrix $\mathbf{W}$ is constructed by multiplying the appropriate permutation matrix from the codebook with a power scaling factor. That is to say, the optimization of $\mathbf{W}$ is replaced by $\sqrt{\beta_l}\mathbf{T}_l$, where β_l is a variable power scaling factor. Thus, each permutation matrix gives rise to a permuted channel matrix for which we can design (by the algorithms developed below) a so-called *latent* transceiver, consisting of the BS beamforming vectors, the RS power scaling factor and the receiver PS ratios. Among the B latent transceivers so obtained, the optimal one with index l_{opt} is chosen by means of a suitable selection criterion for transmission. Specifically, the selection mechanism is designed to choose the optimal latent transceiver with the minimum power consumption, which can be expressed as

$$l_{opt} = \arg\min_{l}\ P_l, \quad (32)$$

where P_l denotes the total transmission power corresponding to the lth latent transceiver.

[5] A permutation matrix is a square binary matrix that has exactly one entry equal to 1 in each row and each column, while all the other entries are equal to 0.

[6] The total number of permutation matrices at the RS is $N_r!$. It is not realistic to use all such permutation matrices as codebook entries when N_r is large. Thus, we propose to construct a codebook of permutation matrices with B elements, where $B \ll N_r!$. In practice, the value of B should be chosen to achieve a suitable tradeoff between performance requirements and implementation complexity. The codebook design approach will be introduced in Subsection IV-D.

Before data transmission, the BS only sends the index of the permutation matrix, the RS power scaling factor and the receiver PS ratios corresponding to the optimum transceiver to the RS and the receivers. Compared to the AO-based algorithms, the SR-based algorithms can significantly reduce the number of signaling bits and the computational complexity. The proposed SR-based scheme works as follows:

- The BS designs the B latent transceivers based on available permutation matrices within the codebook; it then determines the optimal latent transceiver based on (32).
- The BS sends the optimal permutation index l_{opt}, the corresponding RS power scaling factor, and the PS ratios corresponding to the optimal transceiver to the RS and the receivers.
- The RS constructs the optimal RS AF matrix based on the forwarded RS power scaling factor and the stored permutation matrix with index l_{opt}.

We introduce the latent transceiver design algorithms for both perfect and imperfect CSI cases in Subsection IV-A and IV-B, respectively. In Subsection IV-C, a simplified SR-based transceiver design algorithm is proposed. The design approach for the codebook of permutation matrices is presented in Subsection IV-D.

A. Latent Transceiver Design With Perfect CSI

Firstly, we introduce an algorithm to construct the lth latent transceiver with perfect CSI. We aim to design the beamforming vectors $\{\mathbf{f}_k^l\}$, the RS power scaling factor β_l and the receiver PS ratios $\{\rho_k^l\}$ so as to minimize the sum of BS and RS transmit power under both SINR and EH constraints. We note that superscripts l in $\{\mathbf{f}_k^l\}$, $\{\rho_k^l\}$, etc., have been removed in the following for notational simplicity. For each latent transceiver, let $\mathbf{W} \triangleq \sqrt{\beta_l}\mathbf{T}_l$, the optimization problem can be formulated as

$$\begin{aligned} &\min_{\{\mathbf{f}_k,\ \rho_k\},\ \beta_l} \quad P_B + P_R \\ &\text{s.t. } \Gamma_k \geq \gamma_k, \quad P_k^{\text{EH}} \geq \psi_k, \quad 0 \leq \rho_k \leq 1, \quad \forall k \in \mathcal{K}. \end{aligned} \tag{33}$$

As we can see, although we replaced the AF matrix $\mathbf{W}$ with $\sqrt{\beta_l}\mathbf{T}_l$, problem (33) is still non-convex and difficult to solve due to the coupling between variables $\mathbf{f}_k$, ρ_k and β_l. Our proposed method is motivated by the observation that problem (33) can be reformulated as a difference of convex (DC) programming problem with proper transformations. Thus, the concept of CCCP [25], [26] can be adopted to iteratively solve the DC problem, as explained below.

First, we introduce the variable substitution

$$\varphi_l = \frac{1}{\beta_l}, \tag{34}$$

and further define the following vectors:

$$\begin{aligned} &\mathbf{p} = [p_1, \ldots, p_K]^T, \quad \mathbf{q} = [q_1, \ldots, q_K]^T, \\ &\mathbf{f} = [\mathbf{f}_1^T, \ldots, \mathbf{f}_K^T]^T, \quad \mathbf{r} = [\mathbf{p}^T, \mathbf{q}^T, \varphi_l, \mathbf{f}^T]^T, \end{aligned} \tag{35}$$

where p_k and q_k have already been introduced in Subsection III-B, alongside with (24) and (25). Then, the objective function of problem (33) can be transformed into

$$P_l(\mathbf{r}) = \sum_{k=1}^{K} \mathbf{f}_k^H \mathbf{f}_k + \sum_{k=1}^{K} \frac{\mathbf{f}_k^H \mathbf{G}^H \mathbf{G} \mathbf{f}_k}{\varphi_l} + \sigma_r^2 \frac{1}{\varphi_l}, \tag{36}$$

which is strictly jointly convex in the variables $\{\varphi_l, \mathbf{f}\} \in \mathbb{R}_+ \times \mathbb{C}^{KN_t \times 1}$ [22], [41], [42].

Similar to the transformation of the objective function, the SINR constraints can be rewritten as

$$w_k(\mathbf{r}) - x_k(\mathbf{r}) \leq 0, \tag{37}$$

where $w_k(\mathbf{r})$ and $x_k(\mathbf{r})$ are defined as

$$\begin{aligned} w_k(\mathbf{r}) = &\sum_{j \neq k}^{K} \mathbf{f}_j^H \mathbf{G}^H \mathbf{T}_l^H \hat{\mathbf{h}}_k \hat{\mathbf{h}}_k^H \mathbf{T}_l \mathbf{G} \mathbf{f}_j + \sigma_k^2 \varphi_l + \sigma_r^2 \hat{\mathbf{h}}_k^H \hat{\mathbf{h}}_k \\ &+ \frac{1}{4}\omega_k^2 (p_k + \varphi_l)^2, \end{aligned} \tag{38}$$

$$x_k(\mathbf{r}) = \frac{1}{4}\omega_k^2 (p_k - \varphi_l)^2 + \frac{1}{\gamma_k} \mathbf{f}_k^H \mathbf{G}^H \mathbf{T}_l^H \hat{\mathbf{h}}_k \hat{\mathbf{h}}_k^H \mathbf{T}_l \mathbf{G} \mathbf{f}_k. \tag{39}$$

Moreover, the EH constraints can be recast as

$$y_k(\mathbf{r}) - z_k(\mathbf{r}) \leq 0, \tag{40}$$

where

$$y_k(\mathbf{r}) = \frac{\psi_k}{4\xi_k}(q_k + \varphi_l)^2 - \sigma_r^2 \hat{\mathbf{h}}_k^H \hat{\mathbf{h}}_k, \tag{41}$$

$$z_k(\mathbf{r}) = \sum_{j=1}^{K} \mathbf{f}_j^H \mathbf{G}^H \mathbf{T}_l^H \hat{\mathbf{h}}_k \hat{\mathbf{h}}_k^H \mathbf{T}_l \mathbf{G} \mathbf{f}_j + \sigma_k^2 \varphi_l + \frac{\psi_k}{4\xi_k}(q_k - \varphi_l)^2. \tag{42}$$

We remark that (38), (39), (41) and (42) are all jointly convex functions with respect to the variables in $\mathbf{r} \in \mathbb{R}_+^K \times \mathbb{R}_+^K \times \mathbb{R}_+ \times \mathbb{C}^{KN_t \times 1}$. Thus, problem (33) can be equivalently reformulated as the following DC program:

$$\begin{aligned} &\min_{\mathbf{r}} \ P_l(\mathbf{r}) \\ &\text{s.t. } w_k(\mathbf{r}) - x_k(\mathbf{r}) \leq 0, \ y_k(\mathbf{r}) - z_k(\mathbf{r}) \leq 0, \\ &\quad p_k \geq 1, \quad q_k \geq 1, \quad \text{invp}(p_k) + \text{invp}(q_k) \leq 1, \quad \forall k \in \mathcal{K}. \end{aligned} \tag{43}$$

According to the concept of CCCP, we approximate the functions $x_k(\mathbf{r})$ and $z_k(\mathbf{r})$ in the ith iteration by their first-order Taylor expansions around the current point $\mathbf{r}^{(i)}$, denoted as $\hat{x}_k(\mathbf{r}^{(i)}, \mathbf{r})$ and $\hat{z}_k(\mathbf{r}^{(i)}, \mathbf{r})$, respectively. With the help of [43] and [42], $\hat{x}_k(\mathbf{r}^{(i)}, \mathbf{r})$ can be expressed as the following affine function of $\mathbf{r}$:

$$\hat{x}_k(\mathbf{r}^{(i)}, \mathbf{r}) = x_k(\mathbf{r}^{(i)}) + 2\Re\{\nabla x_k(\mathbf{r}^{(i)})^H (\mathbf{r} - \mathbf{r}^{(i)})\}, \tag{44}$$

where $\nabla x_k(\mathbf{r}^{(i)})$ denotes the conjugate derivative of the function $x_k(\mathbf{r})$ with respect to the complex vector $\mathbf{r}$.[7] We note that $\hat{x}_k(\mathbf{r}^{(i)}, \mathbf{r})$ is an affine function of $\mathbf{r}$. $\nabla x_k(\mathbf{r}^{(i)})$ is given by

$$\begin{aligned} \nabla x_k(\mathbf{r}^{(i)}) = \Big[&\mathbf{0}_{1\times(k-1)}, \frac{1}{4}\omega_k^2 (p_k^{(i)} - \varphi_l^{(i)}), \mathbf{0}_{1\times(2K-k)}, \\ &- \frac{1}{4}\omega_k^2 (p_k^{(i)} - \varphi_l^{(i)}), \frac{1}{\gamma_k} (\mathbf{G}^H \mathbf{T}_l^H \hat{\mathbf{h}}_k \hat{\mathbf{h}}_k^H \mathbf{T}_l \mathbf{G} \mathbf{f}_k^{(i)})^T \Big]^T. \end{aligned} \tag{45}$$

[7] Since $\mathbf{r}$ is composed of both real and complex variables, we need to slightly modify $\nabla x_k(\mathbf{r}^{(i)})$ such that (44) holds for $\mathbf{r}$.

Similarly, $\hat{z}_k(\mathbf{r}^{(i)}, \mathbf{r})$ can be expressed as

$$\hat{z}_k(\mathbf{r}^{(i)}, \mathbf{r}) = z_k(\mathbf{r}^{(i)}) + 2\Re\{\nabla z_k(\mathbf{r}^{(i)})^H(\mathbf{r} - \mathbf{r}^{(i)})\}, \quad (46)$$

where

$$\nabla z_k(\mathbf{r}^{(i)}) = [\mathbf{0}_{1\times(K+k-1)}, \frac{\psi_k}{4\xi_k}(q_k^{(i)} - \varphi_l^{(i)}), \mathbf{0}_{1\times(K-k)},$$
$$\frac{1}{2}\sigma_k^2 - \frac{\psi_k}{4\xi_k}(q_k^{(i)} - \varphi_l^{(i)}), \ (\tilde{\mathbf{G}}_k\mathbf{f}_1^{(i)})^T, \ldots, (\tilde{\mathbf{G}}_k\mathbf{f}_K^{(i)})^T]^T, \quad (47)$$
$$\tilde{\mathbf{G}}_k = \mathbf{G}^H\mathbf{T}_l^H\hat{\mathbf{h}}_k\hat{\mathbf{h}}_k^H\mathbf{T}_l\mathbf{G}. \quad (48)$$

Then, in the ith iteration of the proposed CCCP based algorithm, we have the following convex optimization problem:

$$\begin{aligned}\min_{\mathbf{r}} \ & P_l(\mathbf{r}) \\ \text{s.t. } & w_k(\mathbf{r}) - \hat{x}_k(\mathbf{r}^{(i)}, \mathbf{r}) \le 0, \quad y_k(\mathbf{r}) - \hat{z}_k(\mathbf{r}^{(i)}, \mathbf{r}) \le 0, \\ & p_k \ge 1, \quad q_k \ge 1, \quad \text{invp}(p_k) + \text{invp}(q_k) \le 1, \quad \forall k \in \mathcal{K},\end{aligned} \quad (49)$$

whose solution is denoted by $\mathbf{r}^{(i+1)}$.

Proposition 2: By introducing a new set of variables d_k, $\tilde{d}_k$, e_k and $\tilde{e}_k$, $k \in \mathcal{K}$, problem (49) can be reformulated as the following SOCP problem:

$$\begin{aligned}\min_{\mathbf{r},\ P_1,\ P_2,\ P_3} \ & P_1 + P_2 + P_3 \\ \text{s.t. } & \|[\mathbf{f}_1^T, \ldots, \mathbf{f}_K^T, (P_1 - 1)/2]\| \le (P_1 + 1)/2, \\ & \|[(\mathbf{G}\mathbf{f}_1)^T, \ldots, (\mathbf{G}\mathbf{f}_K)^T, (P_2 - \varphi_l)/2]\| \le (P_2 + \varphi_l)/2, \\ & \|[2\sigma_r, \varphi_l - P_3]\| \le \varphi_l + P_3, \\ & \left\|\left[\mathbf{w}_k^T, \frac{\tilde{d}_k - d_k - 1}{2}\right]\right\| \le \frac{\tilde{d}_k - d_k + 1}{2}, \quad \forall k, \\ & \left\|\left[\sqrt{\frac{\psi_k}{4\xi_k}}(q_k + \varphi_l), \frac{\tilde{e}_k - e_k - 1}{2}\right]\right\| \le \frac{\tilde{e}_k - e_k + 1}{2}, \\ & p_k \ge 1, \ q_k \ge 1, \quad \text{invp}(p_k) + \text{invp}(q_k) \le 1, \quad \forall k \in \mathcal{K},\end{aligned} \quad (50)$$

where $\mathbf{w}_k$ is defined in (68).

Proof: Please refer to Appendix C. ∎

We can show that the proposed CCCP based iterative algorithm for the lth transceiver design converges to a local optimal solution of problem (33). The proof is similar to that of *Lemma 2* and *Theorem 1* in [42], and we therefore omit the details. Since the algorithm for the lth transceiver design converges, then based on the selection mechanism (32) we can infer that the whole algorithm converges. We summarize the proposed latent transceiver design algorithm with perfect CSI in Table III.

B. Latent Transceiver Design With Imperfect CSI

Secondly, let us propose a robust latent transceiver design algorithm by taking the channel errors into consideration. As we can see, the concept of SR can also be applied to problem (14), which can be reformulated as follows:

$$\begin{aligned}\min_{\{\mathbf{f}_k,\ \rho_k\},\ \beta_l} \ & P_B + P_R \\ \text{s.t. } & \Gamma_k \ge \gamma_k, \quad P_k^{\text{EH}} \ge \psi_k, \quad 0 \le \rho_k \le 1, \\ & \mathbf{W} = \sqrt{\beta_l}\mathbf{T}_l, \quad \|\mathbf{e}_k\|^2 \le \eta_k^2, \quad \forall k \in \mathcal{K}.\end{aligned} \quad (51)$$

TABLE III

SR Perfect CSI: LATENT TRANSCEIVER DESIGN ALGORITHM WITH PERFECT CSI

1. Define the tolerance of accuracy $\delta > 0$ and the maximum number of iterations N_{max}.
2. **For** $l = 1, \ldots, B$
3. – Initialize the algorithm with a feasible point $\mathbf{r}^{(0)}$. Set the iteration number $i = 0$.
4. – **Repeat**
   – Compute the affine approximation $\hat{x}_k(\mathbf{r}^{(i)}, \mathbf{r})$ and $\hat{z}_k(\mathbf{r}^{(i)}, \mathbf{r})$ according to (44) and (46), respectively.
   – Solve problem (50), and assign the solution to $\mathbf{r}^{(i+1)}$.
   – Update the iteration number : $i = i + 1$.
   – **Until** $|P_l(\mathbf{r}^{(i+1)}) - P_l(\mathbf{r}^{(i)})| \le \delta$ or the maximum number of iterations is reached, i.e., $i > N_{\max}$.
5. – Obtain the lth latent transceiver $\{\mathbf{f}_k^*, \rho_k^*, \beta_l^*\}$.
6. **End**

We employ a subgradient-type iterative algorithm to solve this problem. Our proposed method is motivated by the observation that, if we fix β_l, then problem (51) is equivalent to problem (26) with the SDR technique.[8] With fixed β_l, (24) and (25) can be reformulated as the following two LMIs:

$$\begin{bmatrix} \overline{\mathbf{U}}_k + \lambda_k\mathbf{I} & \overline{\mathbf{U}}_k\hat{\mathbf{h}}_k \\ \hat{\mathbf{h}}_k^H\overline{\mathbf{U}}_k & \hat{\mathbf{h}}_k^H\overline{\mathbf{U}}_k\hat{\mathbf{h}}_k - \frac{\sigma_k^2}{\beta_l} - \frac{\omega_k^2 p_k}{\beta_l} - \lambda_k\eta_k^2 \end{bmatrix} \succeq \mathbf{0}, \quad (52)$$

$$\begin{bmatrix} \overline{\mathbf{V}}_k + \mu_k\mathbf{I} & \overline{\mathbf{V}}_k\hat{\mathbf{h}}_k \\ \hat{\mathbf{h}}_k^H\overline{\mathbf{V}}_k & \hat{\mathbf{h}}_k^H\overline{\mathbf{V}}_k\hat{\mathbf{h}}_k + \frac{\sigma_k^2}{\beta_l} - \frac{\psi_k}{\xi_k\beta_l}q_k - \mu_k\eta_k^2 \end{bmatrix} \succeq \mathbf{0}, \quad (53)$$

where $\overline{\mathbf{U}}_k = \frac{1}{\gamma_k}\tilde{\mathbf{Q}}_k - \sum_{j\ne k}^{K}\tilde{\mathbf{Q}}_j - \sigma_r^2\mathbf{I}$, $\overline{\mathbf{V}}_k = \sum_{j=1}^{K}\tilde{\mathbf{Q}}_j + \sigma_r^2\mathbf{I}$, and $\tilde{\mathbf{Q}}_k = \mathbf{T}_l\mathbf{G}\mathbf{F}_k\mathbf{G}^H\mathbf{T}_l^H$.

Then, with the use of the SDR technique and fixed β_l, problem (51) can be expressed as

$$\begin{aligned} f(\beta_l) = \min_{\{\mathbf{F}_k,\ p_k,\ q_k,\ \lambda_k,\ \mu_k\}} & \sum_{k=1}^{K}\text{Tr}(\mathbf{F}_k) + \beta_l\sum_{k=1}^{K}\text{Tr}(\tilde{\mathbf{Q}}_k) + \sigma_r^2\beta_l \\ \text{s.t. } & (52) \text{ and } (53), \ \lambda_k \ge 0, \ \mu_k \ge 0, \\ & \mathbf{F}_k \succeq \mathbf{0}, \ p_k \ge 1, \quad q_k \ge 1, \\ & \text{invp}(p_k) + \text{invp}(q_k) \le 1, \quad \forall k \in \mathcal{K}. \end{aligned} \quad (54)$$

We here consider the SDR version of problem (51) instead of its original form with rank-one constraints, since strong duality holds if problem (54) is feasible. The partial dual problem of (54) can be formulated as (55) shown at the bottom of next page, where $\mathbf{X}_k = \begin{bmatrix} \overline{\mathbf{X}}_k & \mathbf{x}_k \\ \mathbf{x}_k^H & x_k \end{bmatrix}$ and $\mathbf{Y}_k = \begin{bmatrix} \overline{\mathbf{Y}}_k & \mathbf{y}_k \\ \mathbf{y}_k^H & y_k \end{bmatrix}$ denote the dual variables associated with constraints (52) and (53), respectively. It is worth noting that $\mathbf{X}_k$ and $\mathbf{Y}_k$ can be obtained as side information with any standard SDP solver, since dual variables are served as a certificate for optimality.

Next, we can use the subgradient method [44] to iteratively solve the SDR version of problem (51). At the $(i+1)$th iteration, the power scaling factor β_l can be updated according to

$$\beta_l(i+1) = [\beta_l(i) - \theta(i)s(i)]_{\varepsilon}^{+}, \quad (56)$$

[8]The concept of CCCP can also be applied to the robust problem (51). However, based on simulations we find that the performance of the CCCP based algorithm is inferior to that of the subgradient-type algorithm. Thus, we employ the subgradient-type algorithm instead.

TABLE IV

SR Imperfect CSI: ROBUST LATENT TRANSCEIVER DESIGN ALGORITHM WITH IMPERFECT CSI

1. Initialize the step-size θ, define the tolerance of accuracy $\delta > 0$ and the maximum number of iterations N_{max}.
2. **For** $l = 1, \ldots, B$
3. – Initialize $\beta_l(0)$. Set the iteration number $i = 0$.
4. – **Repeat**
   – Solve problem (54) to obtain the optimal $\{\mathbf{F}_k^*, \rho_k^*\}$ and the corresponding dual variables $\{x_k^*, y_k^*\}$.
   – Update the power scaling factor according to (56).
   – Update the iteration number : $i = i + 1$.
   – **Until** $|f(\beta_l(i+1)) - f(\beta_l(i))| \leq \delta$ or the maximum number of iterations is reached, i.e., $i > N_{\max}$.
5. – Obtain the lth latent transceiver $\{\mathbf{f}_k^*, \rho_k^*, \beta_l^*\}$.
6. **End**

where $[\cdot]_{\varepsilon}^{+} = \max(., \varepsilon)$, $\theta(i)$ is the step-size in the ith iteration and $s(i)$ denotes a subgradient of $f(\beta_l)$ at $\beta_l(i)$. The subgradient $s(i)$ can be calculated as [45]

$$s(i) = \sum_{k=1}^{K} \mathrm{Tr}(\tilde{\mathbf{Q}}_k^*) + \sigma_r^2 - \sum_{k=1}^{K} x_k^* \Big(\frac{\sigma_k^2}{\beta_l(i)^2} + \frac{\omega_k^2}{\rho_k^* \beta_l(i)^2} \Big) + \sum_{k=1}^{K} y_k^* \Big(\frac{\sigma_k^2}{\beta_l(i)^2} - \frac{\psi_k}{(1-\rho_k^*)\xi_k \beta_l(i)^2} \Big), \quad (57)$$

where $\tilde{\mathbf{Q}}_k^* = \mathbf{T}_l \mathbf{G} \mathbf{F}_k^* \mathbf{G}^H \mathbf{T}_l^H$, $\{\mathbf{F}_k^*, \rho_k^*\}$ denotes the optimal solution of problem (54) and $\{x_k^*, y_k^*\}$ denote the lower right corner elements of $\mathbf{X}_k^*$ and $\mathbf{Y}_k^*$, which are the optimal dual variables associated with (52) and (53).

Finally, the robust latent transceiver design algorithm is summarized in Table IV.[9]

C. Proposed Simplified SR-Based Transceiver Design

As explained in Subsection IV-A and IV-B, the proposed SR-based transceiver design algorithms involve devising B latent transceivers corresponding to the elements in Υ where for each transceiver, we employ iterative methods to address the highly non-convex problem. Specifically, the design of each transceiver involves an iterative algorithm to obtain the corresponding BS beamforming vectors, RS power scaling factor and receiver PS ratios. However, for given CSIs only the best transceiver with the minimum total power consumption is selected for transmission according to the selection mechanism (32) while the other $B - 1$ solutions are discarded. Thus, there will be a considerable waste in the computational resources. In order to improve the proposed SR-based transceiver design algorithm and make it more suitable for practical implementation, we propose a heuristic approach, referred to as the *simplified* latent transceiver design algorithm, to address the aforementioned problem. Based on simulation experiments, we find that an initial point obtained by solving problem (33) or (51) with fixed initial power scaling factor β_l almost always leads to a better solution after convergence, than by iteratively solving starting from some other initial points. Thus, we only design the particular transceiver with the best initial point.

[9]For the perfect CSI case, we can also employ the subgradient method to address problem (33), with each subproblem being treated as an SDP problem. It is well known that solving an SDP problem requires relatively high computational complexity compared with solving an SOCP problem. Moreover, it is important to note that the two algorithms (i.e., CCCP versus subgradient) for the perfect CSI case exhibit very close performance in our simulations. Thus, we employ the CCCP based algorithm for the perfect CSI case.

TABLE V

Simplified SR Perfect CSI: SIMPLIFIED LATENT TRANSCEIVER DESIGN ALGORITHM WITH PERFECT CSI

1. Define the tolerance of accuracy $\delta > 0$ and the maximum number of iterations N_{max}.
2. **For** the lth latent transceiver ($l = 1, \ldots, B$)
3. – Compute an initial feasible point $\mathbf{r}^{(0)}$ which is obtained by solving problem (33) with $\mathbf{W} = \mathbf{T}_l$.
4. **end**
5. Choose the initial $\mathbf{r}^{(0)}$ and $\mathbf{T}_{l_{opt}}$ with the minimum objective value. Set the iteration number $i = 0$.
6. **Repeat**
   – Compute the affine approximation $\hat{x}_k(\mathbf{r}^{(i)}, \mathbf{r})$ and $\hat{z}_k(\mathbf{r}^{(i)}, \mathbf{r})$ according to (44) and (46), respectively.
   – Solve problem (50), and assign the solution to $\mathbf{r}^{(i+1)}$.
   – Update the iteration number : $i = i + 1$.
7. **Until** $|P_{l_{opt}}(\mathbf{r}^{(i+1)}) - P_{l_{opt}}(\mathbf{r}^{(i)})| \leq \delta$ or the maximum number of iterations is reached, i.e., $i > N_{\max}$.

The proposed simplified latent transceiver design algorithm with perfect CSI is summarized in Table V. The robust version of the simplified latent transceiver design algorithm can be obtained in a similar manner as for the perfect CSI case, and thus is omitted here. We will show in Section VI that the simplified SR-based transceiver design algorithms can achieve a similar performance with that of the proposed SR-based algorithms in Table III and IV.

D. Codebook Design

In this subsection, we propose two simple algorithms to construct the codebook of permutation matrices. The basic

$$f(\beta_l) = \max_{\{\mathbf{X}_k, \mathbf{Y}_k\}} \min_{\{\mathbf{F}_k, \rho_k\}} - \sum_{k=1}^{K} \mathrm{Tr}\Bigg(\mathbf{X}_k \begin{bmatrix} \overline{\mathbf{U}}_k + \lambda_k \mathbf{I} & \overline{\mathbf{U}}_k \hat{\mathbf{h}}_k \\ \hat{\mathbf{h}}_k^H \overline{\mathbf{U}}_k & \hat{\mathbf{h}}_k^H \overline{\mathbf{U}}_k \hat{\mathbf{h}}_k - \frac{\sigma_k^2}{\beta_l} - \frac{\omega_k^2 a_k}{\beta_l} - \lambda_k \eta_k^2 \end{bmatrix} \Bigg) - \sum_{k=1}^{K} \mathrm{Tr}\Bigg(\mathbf{Y}_k \begin{bmatrix} \overline{\mathbf{V}}_k + \mu_k \mathbf{I} & \overline{\mathbf{V}}_k \hat{\mathbf{h}}_k \\ \hat{\mathbf{h}}_k^H \overline{\mathbf{V}}_k & \hat{\mathbf{h}}_k^H \overline{\mathbf{V}}_k \hat{\mathbf{h}}_k + \frac{\sigma_k^2}{\beta_l} - \frac{\psi_k}{\xi_k \beta_l} \beta_k - \mu_k \eta_k^2 \end{bmatrix} \Bigg) + \sum_{k=1}^{K} \mathrm{Tr}(\mathbf{F}_k) + \beta_l \sum_{k=1}^{K} \mathrm{Tr}(\tilde{\mathbf{Q}}_k) + \sigma_r^2 \beta_l, \quad (55)$$

TABLE VI
COMPLEXITY ANALYSIS OF THE PROPOSED TRANSCEIVER DESIGNS

Algorithms	Complexity Order (suppressing the $\ln(1/\varepsilon)$)
AO perfect CSI	$I_1(\mathcal{O}(n_1\sqrt{KN_t}(KN_t^3+n_1KN_t^2+n_1^2))+\mathcal{O}(n_2N_r(N_r^6+n_2N_r^4+n_2^2)))$, $n_1=\mathcal{O}(KN_t^2+K)$, $n_2=\mathcal{O}(N_r^4)$.
AO imperfect CSI	$I_2(\mathcal{O}(n_1\sqrt{2K(N_r+1)+KN_t}(2K(N_r+1)^3+KN_t^3+2n_1K(N_r+1)^2+n_1KN_t^2+n_1^2))$ $+\mathcal{O}(n_2\sqrt{2K(N_r+1)+N_r^2}(2K(N_r+1)^3+N_r^6+2n_2K(N_r+1)^2+n_2N_r^4+n_2^2))$ $+R(\mathcal{O}(2K\sqrt{4K}(18K+4K^2))))$, $n_1=\mathcal{O}(KN_t^2+4K)$, $n_2=\mathcal{O}(N_r^4+2K)$.
SR perfect CSI	$BI_3(\mathcal{O}(n\sqrt{4K+6}((KN_t+2)^2+(KN_r+2)^2+K(K+2)^2+9(K+1)+n^2)))$, $n=\mathcal{O}(KN_t+2K)$.
SR imperfect CSI	$BI_4(\mathcal{O}(n_1\sqrt{2K(N_r+1)+KN_t}(2K(N_r+1)^3+KN_t^3+2n_1K(N_r+1)^2+n_1KN_t^2$ $+n_1^2))+R(\mathcal{O}(2K\sqrt{4K}(18K+4K^2))))$, $n_1=\mathcal{O}(KN_t^2+4K)$.
Simplified SR perfect CSI	$(B+I_3)(\mathcal{O}(n\sqrt{4K+6}((KN_t+2)^2+(KN_r+2)^2+K(K+2)^2+9(K+1)+n^2)))$, $n=\mathcal{O}(KN_t+2K)$.
Simplified SR imperfect CSI	$(B+I_4)(\mathcal{O}(n_1\sqrt{2K(N_r+1)+KN_t}(2K(N_r+1)^3+KN_t^3+2n_1K(N_r+1)^2$ $+n_1KN_t^2+n_1^2))+R(\mathcal{O}(2K\sqrt{4K}(18K+4K^2))))$, $n_1=\mathcal{O}(KN_t^2+4K)$.

principle of the proposed algorithms is to choose the permutation matrices which are more likely to result in lower transmission power. Define $\mathbf{H}=[\mathbf{h}_1,\ldots,\mathbf{h}_K]^H$ and let $\mathbf{HT}_l\mathbf{G}$ represent the equivalent channel matrix between the BS and the K receivers. Based on several numerical experiments, we make the essential observation that when the singular values of the permuted channel matrix $\mathbf{HT}_l\mathbf{G}$ are either larger or more equally distributed, the total power consumption is usually smaller.

Let π_k^l denote the kth singular value of $\hat{\mathbf{H}}\mathbf{T}_l\mathbf{G}$, $k\in\mathcal{K}$, where $\hat{\mathbf{H}}=[\hat{\mathbf{h}}_1,\ldots,\hat{\mathbf{h}}_K]^H$. The first scheme (referred to as *Sum-Max* method) constructs the codebook of permutation matrices by choosing the ones which correspond to the B largest sums of singular values, i.e.,

$$\{\mathbf{T}_1,\ldots,\mathbf{T}_B\}=\arg\max_{\mathbf{T}_l}\text{B}\ \left(\sum_{k=1}^{K}\pi_k^l\right), \tag{58}$$

where maxB$(\cdot)$ returns the permutation matrices correspond to the B largest values of its argument.

Alternatively, the second scheme (referred to as *Max-Min* method) chooses the permutation matrices to maximize the smallest singular value, i.e.,

$$\{\mathbf{T}_1,\ldots,\mathbf{T}_B\}=\arg\max_{\mathbf{T}_l}\text{B}\ \left(\min_{k\in\mathcal{K}}(\pi_k^l)\right). \tag{59}$$

It is worth noting that the proposed two schemes are heuristic techniques which may serve as a shortcut to the process of finding a satisfactory solution. The comparative performance of these two codebook design algorithms will be studied as part of the simulation experiments reported in Section VI.

V. COMPUTATIONAL COMPLEXITY

In Section III and IV, we proposed the AO-based and SR-based transceiver design algorithms for problem (13) and (14), respectively. In this section, we compare the relative computational complexity of the proposed transceiver design algorithms. To this end, we apply the same basic element of complexity analysis as in [46]. Among the proposed algorithms in this paper, we consider the following: *AO perfect CSI*, *AO imperfect CSI*, *SR perfect CSI*, *SR imperfect CSI*, *Simplified SR perfect CSI* and *Simplified SR imperfect CSI* (the robust counterpart of the algorithm in Table V).

The complexity of the *AO perfect CSI* algorithm is dominated by solving problems (15) and (20) I_1 times, where I_1 denotes the number of iterations. We note that the dual problems of (15) and (20) can be solved instead of (15) and (20) for better efficiency. Consider the dual problem of (15), which involves K LMI constraints of size N_t and on the order of $n_1=O(KN_t^2+K)$ decision variables. Thus, the complexity of a generic interior-point method for solving problem (15) is given by $O(n_1\sqrt{KN_t}(KN_t^3+n_1KN_t^2+n_1^2))$. Similarly, the complexity of solving the dual problem of (20) can be written as $O(n_2\sqrt{N_r^2}(N_r^6+n_2N_r^4+n_2^2))$, where $n_2=O(N_r^4)$ is the order of the corresponding decision variables. The complexity of solving problem (66) can be neglected since it admits a closed-form solution. Thus, the overall complexity of the *AO perfect CSI* algorithm is on the order of the quantity shown in the first row of Table VI.

The complexity of the *AO imperfect CSI* algorithm is dominated by solving problems (26) and (31) I_2 times, plus the complexity of the rank-one recovery method. Problem (26) involves KN_t^2+4K variables, $2K$ LMI constraints of size N_r+1 and K LMI constraints of size N_t. Problem (31) involves N_r^4+2K variables, $2K$ LMI constraints of size N_r+1 and 1 LMI constraint of size N_r^2. Moreover, the complexity of the rank-one recovery method is dominated by solving problem (65) R times, where R is the number of randomization steps.[10] Problem (65) involves $2K$ variables and $2K$ second-order cone (SOC) constraints of dimension 3. Thus, the overall complexity of the *AO imperfect CSI* algorithm is on the order of the quantity shown in the second row of Table VI.

The complexity of the *SR perfect CSI* algorithm is dominated by solving problem (50) BI_3 times, where I_3 is the iteration number, since the complexity of computing the affine approximation $\hat{x}_k(\mathbf{r}^{(i)},\mathbf{r})$ and $\hat{z}_k(\mathbf{r}^{(i)},\mathbf{r})$ is negligible compared to solving (50). Problem (50) involves $2K+3$ SOC constraints, including 1 SOC of dimension KN_t+2, 1 SOC of dimension KN_r+2, K SOCs of dimension $K+2$, and $K+1$ SOCs of dimension 3. The number of variables is on the order of $O(KN_t+2K)$. It follows that the complexity of

[10]The complexity to recover $\mathbf{W}^*$ is negligible since problem (66) admits a closed-form solution.

the *SR perfect CSI* algorithm is on the order of the quantity shown in the third row of Table VI.

The complexity of the *SR imperfect CSI*, *simplified SR perfect CSI* and *simplified SR imperfect CSI* algorithms can be analyzed in a similar way; the corresponding complexity figures are shown in the fourth to sixth rows of Table VI, respectively, where I_4 denotes the iteration number of the *(simplified) SR imperfect CSI* algorithm.

It is of interest to investigate the asymptotic complexity of the proposed algorithms when N_t, N_r and K are large, i.e., when we let $N_r = N_t = K \to \infty$. We further assume that $I_1 = I_2 = I_3 = I_4 = I$ for simplicity. Under these conditions, one can verify that the complexities of the proposed algorithms in Table VI are on the orders of $2IN_t^{13}$, $2\sqrt{3}IN_t^{13}$, $6BIN_t^{6.5}$, $3\sqrt{3}BIN_t^{10}$, $6(B+I)N_t^{6.5}$ and $3\sqrt{3}(B+I)N_t^{10}$, respectively. As seen, the robust algorithms always consume more computational resources than their non-robust counterparts, the SR-based algorithms have lower complexity compared with the AO-based algorithms and the simplified SR-based algorithms have the lowest complexity.

VI. Simulation Results

In order to evaluate the performance of the proposed transceiver designs, numerical results have been obtained by performing computer simulations. The default system configuration is defined by the following choice of parameters: $N_t = N_r = 4$, $K = 4$, $\xi = 1$, $\sigma_k^2 = \sigma^2 = -70$dBm, $\omega_k^2 = \omega^2 = -50$dBm, and $\sigma_r^2 = -70$dBm unless otherwise specified. In addition, we assume equal SINR and EH thresholds at the destination receivers, i.e., $\gamma_k = \gamma$, $\psi_k = \psi$, $\forall k \in \mathcal{K}$, and equal norm bounds for the second phase channel error vectors, i.e., $\eta_{kj} = \eta$, $\forall j, k$ for simplicity. In the simulations, we assume that the first phase channel coefficients are flat-fading i.i.d. with Rayleigh distribution. The path loss from the source to the relay is set as -60dB, which may correspond to a separation distance around 30 meters with carrier frequency at 900MHz [47]. The signal attenuation from the relay to all mobile receivers is 40dB corresponding to an identical distance of about 5 meters. With this transmission distance, the line-of-sight (LOS) signal is dominant, and thus we use the Rician fading to model the second phase channel [48]. Specifically, $\hat{\mathbf{h}}_k$ can be expressed as

$$\hat{\mathbf{h}}_k = \sqrt{\frac{K_R}{1+K_R}}\hat{\mathbf{h}}_k^{LOS} + \sqrt{\frac{1}{1+K_R}}\hat{\mathbf{h}}_k^{NLOS}, \qquad (60)$$

where $\hat{\mathbf{h}}_k^{LOS} \in \mathbb{C}^{N_r \times 1}$ is the LOS deterministic component and $\hat{\mathbf{h}}_k^{NLOS}$ denotes the Rayleigh fading component with each element being a circularly symmetric complex Gaussian (CSCG) random variable with zero mean and variance of -40dB, while K_R is the Rician factor set to be 2dB. Note that for the LOS component, we use the far-field uniform linear antenna array model with $\hat{\mathbf{h}}_k^{LOS} = 10^{-2}\left[1, e^{j\theta_k}, e^{j2\theta_k}, \ldots, e^{j(N_r-1)\theta_k}\right]$ and $\theta_k = -2\pi d\frac{\sin(\varphi_k)}{\lambda}$, where d is the spacing between successive antenna elements at the RS, λ is the carrier wavelength, and φ_k is the direction of receiver k with a reference axis at the RS. We set $d = \lambda/2$, and $[\varphi_1, \varphi_2, \varphi_3, \varphi_4] = [-30°, -60°, 60°, 30°]$. In the implementation of the proposed

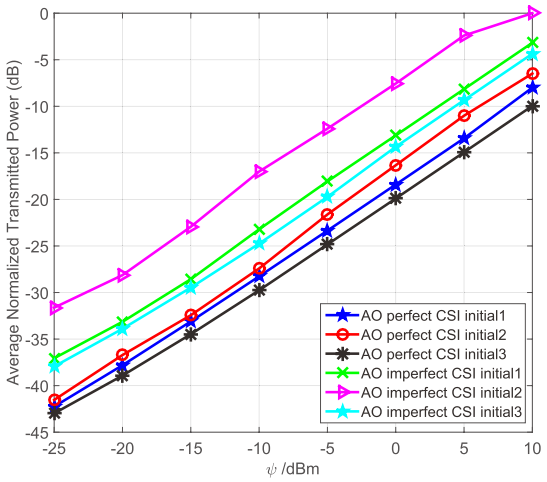

Fig. 3. Comparison of the initialization methods in the AO-based transceiver designs ($\eta = 10^{-3}$, $\gamma = 10$dB).

algorithms, the tolerance parameter is chosen as $\delta = 2 \times 10^{-3}$ while $I_1 = I_2 = 20$ and $I_3 = I_4 = 50$; all the rank-one recovery methods employ $R = 1000$ randomization steps. All convex problems are solved by CVX [49] on a desktop Intel (i3-2100) CPU running at 3.1GHz with 4GB RAM.

In the AO-based transceiver design algorithms, the RS AF matrices $\mathbf{W}$ is initialized in three different ways:

- *Init-1:* Using an identity matrix.
- *Init-2:* Using random matrices drawn from a CSCG distribution with zero mean and unit variance.
- *Init-3:* Using the SR-based transceiver, as explained in Section III and IV.

Fig. 3 shows the average power consumption performance versus the receiver EH target ψ for the AO-based transceiver designs with the three different initialization methods. From the results, we can see that the best performance is achieved by *Init-3* for both perfect and imperfect CSI algorithms, followed by *Init-2* and *Init-1*. For example, the power consumption of *Init-3* is about 1dB less than that of *Init-1* and *Init-2* for the perfect CSI case, and the power saving rises up to 7dB for the imperfect CSI case. As seen, the AO-based algorithms are sensitive to the initial point. The use of *Init-3* is not realistic in practice since it resorts to the SR-based algorithms for initialization. Intuitively, taking the SR-based transceiver as an initial solution can indeed lead to a better performance of the AO-based algorithm since the initial RS AF matrix has been optimized. An optimized $\mathbf{W}$ is most likely to result in a better performance of the AO-based algorithm after convergence, than a randomly generated or unoptimized $\mathbf{W}$. However, in the following simulations, we employ *Init-3* as the initialization method for the AO algorithms under both perfect and imperfect CSI cases, which serves as a performance bound unless otherwise stated. It is also seen from Fig. 3 that the required transmit power for the imperfect CSI scheme is larger than the perfect CSI scheme, which is the price paid for added robustness in the case of imperfect CSI (this will be further illustrated in Fig. 10 and 11).

Note that in the AO-based algorithms (problem (20), (26), (31)), the rank-one recovery methods in Appendix A must be employed to recover rank-one solutions from possibly

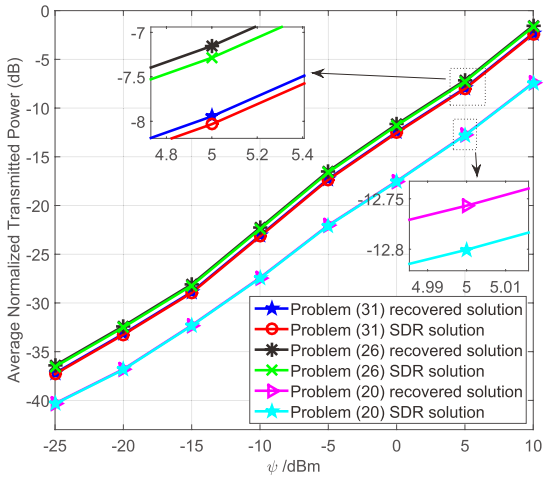

Fig. 4. Performance comparison of the recovered rank-one solution with the modified randomization method and unprocessed SDR solutions in the AO-based transceiver designs ($\eta = 10^{-3}$, $\gamma = 10$dB).

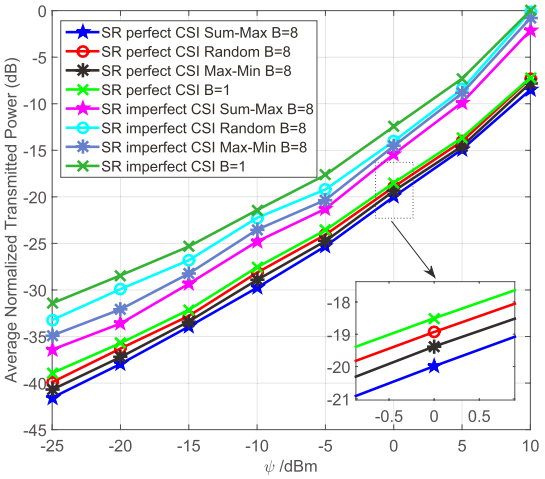

Fig. 6. Comparison of the codebook design methods for the SR-based transceiver designs ($\eta = 10^{-3}$, $\gamma = 10$dB, $\beta_l(0) = 1$, $\theta = 0.1$).

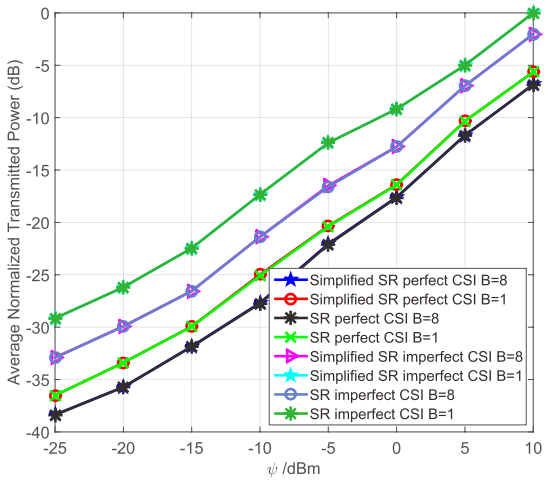

Fig. 5. Performance comparison of the non-simplified and simplified SR-based transceiver designs ($\eta = 10^{-3}$, $\gamma = 10$dB, $\beta_l(0) = 1$, $\theta = 0.1$).

higher rank solutions. In Fig. 4, we show the performance gap between the rank-one recovered solutions and the unprocessed SDR solutions for 20 particular problem instances where higher rank solutions are returned. It can be observed that the performance gap is only about 0.1dB, which means that the recovery methods in Appendix A are very efficient. The corresponding performance gap of problem (54) is similar to that of (31), thus it is not displayed in the figure.

Fig. 5 shows the performance comparison of the SR-based transceiver design algorithms proposed in Subsection IV-A and IV-B and the simplified SR-based transceiver design proposed in Subsection IV-C. It is worth noting that the algorithms with codebook size $B = 1$ only use the identity matrix as the permutation matrix (naive method),[11] and the algorithms with the $B = 8$ codebook employ the *Sum-Max* codebook design method. We include the identity matrix into the $B = 8$ codebook regardless of the singular values in order to guarantee that the performance of the algorithms with $B = 8$ is always better than with $B = 1$. We can see that the simplified SR-based transceiver design algorithms achieve almost the same performance as the non-simplified ones for both perfect and imperfect CSI cases. However, the simplified SR-based algorithms consume much less computational resources compared with their non-simplified counterparts. Thus, we employ the simplified SR-based design in the following simulations for comparison unless otherwise specified.

Next, we compare the performance of the codebook design approaches, i.e., the *Sum-Max* and *Max-Min* methods, in terms of the average power consumption. For completeness, we also consider the performance of a codebook whose elements (permutation matrices) are randomly selected. The results are presented in Fig. 6, which shows the average power consumption performance curves versus EH target. We can see that the *Sum-Max* method outperforms other methods. Compared with the randomly generated codebook, the proposed *Sum-Max* method can lead to a power saving of 1dB for the perfect CSI case and 2dB for the imperfect CSI case. The performance of the *Max-Min* method is slightly inferior to the *Sum-Max* method.

Fig. 7 shows the average power consumption performance for various codebook sizes in the SR-based transceiver design algorithms. It is observed that the robust designs for imperfect CSI with codebook sizes $B = 4, 8, 16$ and 24 achieve a power saving of about 5dB compared to that with the $B = 1$ codebook, while the non-robust designs with perfect CSI and with codebook sizes of $B = 4, 8, 16$ and 24 achieve about 1dB in power saving compared with the $B = 1$ codebook.[12] We can also see from this figure that an increase in B does not necessarily gives rise to an improvement of the power consumption performance when $B > 8$, which is the reason we proposed to construct a restricted number of transceivers,

[11]The naive method means that the RS only processes the received data vector $\mathbf{y}_R$ by adjusting its power (i.e. scaling) and forwarding it.

[12]Note that the algorithms with the $B = 24$ codebook conduct a search for all the $N_r! = 4!$ permutation matrices, which is referred to here as the optimal SR-based transceiver design algorithms.

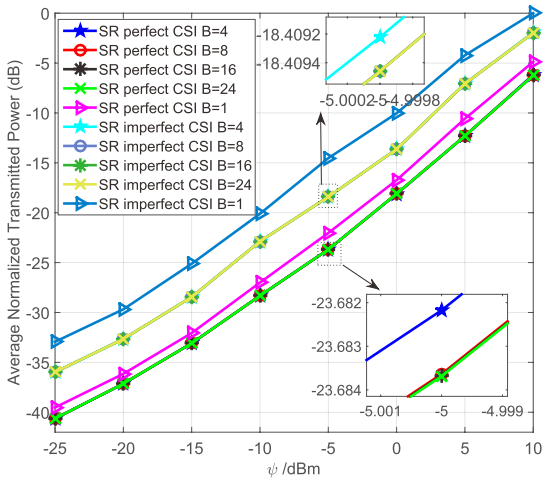

Fig. 7. Codebook size comparison of the SR-based transceiver designs ($\eta = 10^{-3}$, $\gamma = 10$dB, $\beta_l(0) = 1$, $\theta = 0.1$).

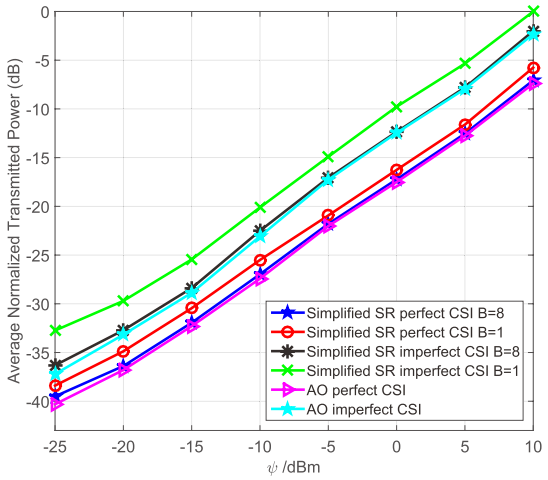

Fig. 8. Performance comparison of the SR-based and AO-based transceiver designs versus ψ. ($\eta = 10^{-3}$, $\gamma = 10$dB, $\beta_l(0) = 1$, $\theta = 0.1$).

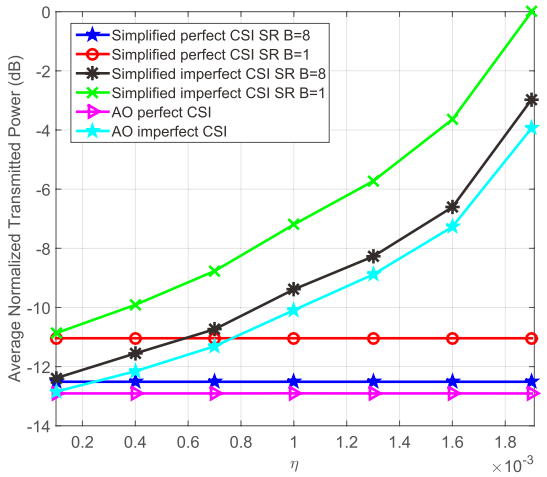

Fig. 9. Performance comparison of the SR-based and AO-based transceiver designs versus η. ($\psi = -5$dBm, $\gamma = 10$dB, $\beta_l(0) = 1$, $\theta = 0.1$).

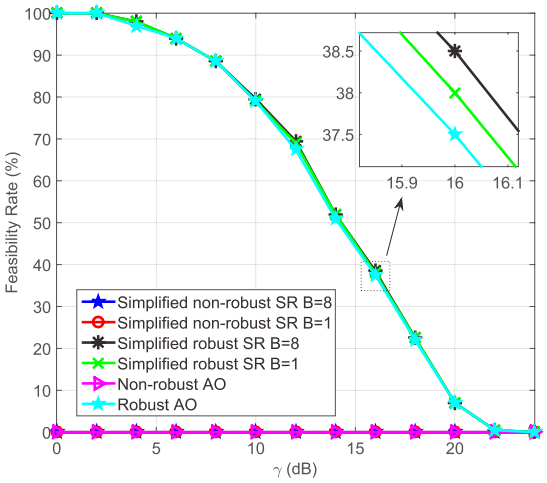

Fig. 10. Feasibility rate comparison of the SR-based and AO-based transceiver designs versus SINR threshold γ ($\psi = 5$dBm, $\eta = 10^{-3}$, $\beta_l(0) = 1$, $\theta = 0.1$).

i.e., to select a small fraction of all the permutation matrices for transceiver design ($B \ll N_r!$).

In the next series of simulations, we examine the comparative performance of the AO-based and SR-based transceiver design algorithms. Fig. 8 shows the average normalized transmitted power versus EH threshold ψ for these two algorithms. It is observed that the performance of the SR-based algorithms is very close to that of the AO-based algorithms. From the complexity analysis in Section V, we note that if N_r increases, the complexity of solving problem (20) and (31) in the AO-based transceiver design algorithms might become unacceptable, which limits the practicality of these algorithms. Thus, the SR-based transceiver design is very promising and suitable for systems with large N_r. It is also important to mention that the number of signaling bits required for the SR-based MISO relay system is much less than that for the AO-based counterpart since only the index of the optimal transceiver and the power scaling factor have to be sent to the RS instead of the whole RS AF matrix.

In Fig. 9, we illustrate the performance of the AO-based and SR-based transceiver design algorithms in terms of the channel error bound η. It can be observed that as η increases, the power consumption of the algorithms with perfect CSI does not change. For the algorithms with imperfect CSI, we can see that their power consumption increases with η, which means that more power is needed to ensure the robustness against channel errors. Also, the performance of the SR-based algorithms are very close to that of the AO-based algorithms.

Finally, a comparison of the feasibility rate between the AO-based and SR-based design algorithms is provided. We consider the following two cases:

- *Robust:* the proposed transceiver design algorithms, which take into account the estimated CSI along with the error bound (i.e., solving problem (14)).
- *Non-robust:* the proposed transceiver design algorithms, which takes into account only the estimated CSI, without consideration of the estimation errors.

Fig. 10 compares the feasibility rate versus SINR target γ for these two cases. One can observe that the feasibility rate performance of the AO-based algorithms is slightly inferior to that of the SR-based algorithms since we employ *Init-3* as the initialization method for the former. Fig. 11 presents a similar

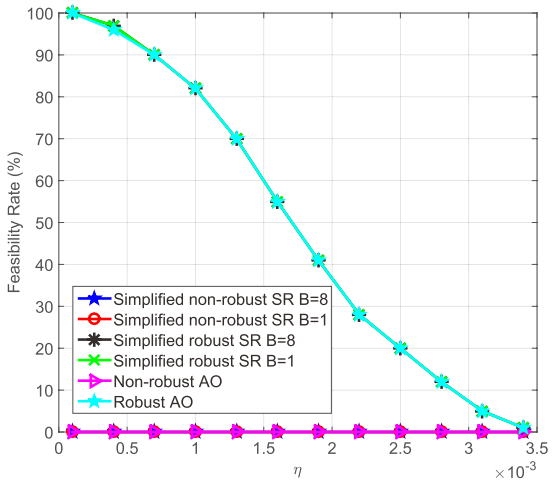

Fig. 11. Feasibility rate comparison of the SR-based and AO-based transceiver designs versus CSI error bound η ($\gamma = 10$dB, $\psi = 5$dBm, $\beta_l(0) = 1$, $\theta = 0.1$).

comparison of the feasibility rate versus the channel error bound η. From this figure, we can see that the performance of the AO-based algorithms is very close to that of the SR-based algorithms. The non-robust algorithms fail to satisfy both the SINR and EH constraints almost all the time under the NBE model, which further motivating the importance of the robust design approach in practice.

VII. Conclusion

In this paper, we considered the joint transceiver design problem for multiuser MISO relay systems with energy harvesting. We proposed AO-based and SR-based algorithms, including both non-robust and robust versions to CSI errors, for the joint optimization of the BS beamforming vectors, the RS AF matrix and the receiver PS ratios. Especially, the SR-based algorithms can achieve almost the same performance compared with the AO-based algorithms but with much reduced computational complexity and overhead. We also presented a simplified SR-based algorithm and carried out a detailed complexity analysis of all the proposed algorithms. Two efficient approaches for the design of the permutation matrix codebook in the SR-based algorithms were proposed. The simulation results validated the effectiveness of the proposed joint transceiver design algorithms and the necessity of using a robust formalism in the presence of imperfect CSI. We remark that the proposed algorithms can be easily extended without significant difficulty to the more elaborate multi-hop relay MISO systems. Furthermore, alternative formulations of the transceiver design, such as energy efficiency maximization, joint uplink-downlink power minimization or joint user scheduling and power minimization, can also be considered. All these remain as open avenues for future work.

Appendix A
Proposed Rank-One Recovery Method

As we mentioned in Section III and IV, the optimal solution of problem (20), (26), (31) and (54) is not guaranteed to be rank-one. In this appendix, we propose a rank-one recovery method based on a randomization procedure. Inspired by the concept of worst-case robustness [50]–[52], we consider the following subproblems:

$$u_{kj} = \min_{\|\mathbf{e}_k\|^2 \le \eta_k^2} |(\hat{\mathbf{h}}_k^H + \mathbf{e}_k^H)\mathbf{W}^*\mathbf{G}\mathbf{f}_j^*|^2, \tag{61}$$

$$v_{kj} = \max_{\|\mathbf{e}_k\|^2 \le \eta_k^2} |(\hat{\mathbf{h}}_k^H + \mathbf{e}_k^H)\mathbf{W}^*\mathbf{G}\mathbf{f}_j^*|^2, \quad j \ne k, \tag{62}$$

$$\overline{w}_k = \max_{\|\mathbf{e}_k\|^2 \le \eta_k^2} \|(\hat{\mathbf{h}}_k^H + \mathbf{e}_k^H)\mathbf{W}^*\|^2, \tag{63}$$

$$\tilde{w}_k = \min_{\|\mathbf{e}_k\|^2 \le \eta_k^2} \|(\hat{\mathbf{h}}_k^H + \mathbf{e}_k^H)\mathbf{W}^*\|^2, \tag{64}$$

where $\mathbf{f}_k^*$ and $\mathbf{W}^*$ are extracted from the optimal solutions $\mathbf{F}_k^*$ and $\tilde{\mathbf{W}}^*$ using the randomization procedure as will be detailed in Table VII.[13] It is not difficult to see that problem (61)-(64) can be solved by the Cauchy-Schwarz inequality and Lagrange multiplier method. We omit the detailed derivation and let $\{u_{kj}^*, v_{kj}^*, \overline{w}_k^*, \tilde{w}_k^*\}$ denote the corresponding optimal objective values.

For problem (26) and (54), we propose to scale up $\mathbf{f}_k^*$ by $\sqrt{\varphi_k}$ and then jointly optimize $\{\sqrt{\varphi_k}\}$ and $\{\rho_k\}$ to recover a rank-one solution. The optimization problem can be reformulated as the following SOCP problem:

$$\begin{aligned}
\min_{\{\varphi_k,\,\rho_k\}} \; & \sum_{k=1}^K \varphi_k \mathbf{f}_k^{*H}\mathbf{f}_k^* + \sum_{k=1}^K \varphi_k \|\mathbf{W}^*\mathbf{G}\mathbf{f}_k^*\|^2 \\
\text{s.t.} \; & \|[2\omega_k,\, z_k - \rho_k]\| \le z_k + \rho_k, \\
& \|[2\sqrt{\psi_k/\xi_k},\, \tilde{z}_k - 1 + \rho_k]\| \le \tilde{z}_k + 1 - \rho_k, \\
& z_k = \frac{\varphi_k u_{kk}^*}{\gamma_k} - \sum_{j\ne k}^K \varphi_j v_{kj}^* - \sigma_k^2 - \sigma_r^2 \overline{w}_k^*, \\
& \tilde{z}_k = \sum_{j=1}^K \varphi_j u_{kj}^* + \sigma_r^2 \tilde{w}_k^* + \sigma_k^2, \\
& \varphi_k \ge 0,\; 0 \le \rho_k \le 1, \quad \forall k \in \mathcal{K}.
\end{aligned} \tag{65}$$

Similarly, we also propose to scale up $\mathbf{W}^*$ by $\sqrt{\varphi}$ and then jointly optimize $\{\sqrt{\varphi}\}$ and $\{\rho_k\}$ to recover a rank-one solution for problem (20) and (31). The optimization problem can be formulated as[14]

$$\begin{aligned}
\min_{\{\varphi,\rho_k\}} \; & \sum_{k=1}^K \varphi \|\mathbf{W}^*\mathbf{G}\mathbf{f}_k^*\|^2 + \sigma_r^2 \varphi \|\mathbf{W}^*\|^2 \\
\text{s.t.} \; & \frac{\rho_k \varphi u_{kk}^*}{\rho_k \varphi \sum\limits_{j\ne k}^K v_{kj}^* + \varphi \rho_k \sigma_r^2 \overline{w}_k^* + \rho_k \sigma_k^2 + \omega_k^2} \ge \gamma_k, \\
& \varphi \sum_{j=1}^K u_{kj}^* + \varphi \sigma_r^2 \tilde{w}_k^* + \sigma_k^2 \ge \frac{\psi_k}{\xi_k(1-\rho_k)}, \\
& \varphi \ge 0,\; 0 \le \rho_k \le 1, \quad \forall k \in \mathcal{K}.
\end{aligned} \tag{66}$$

[13]For problem (54), $\mathbf{W}^*$ can be expressed as $\sqrt{\beta_l^*}\mathbf{T}_l$, where β_l^* denotes the relay power scaling factor corresponding to the lth latent transceiver.

[14]For problem (20), $\{u_{kj}^*, v_{kj}^*, \overline{w}_k^*, \tilde{w}_k^*\}$ is the solution of (61)-(64) with $\mathbf{e}_k = \mathbf{0}$, $\forall k$.

TABLE VII
PROPOSED RANK-ONE RECOVERY METHOD

1. **For** the ith randomization step ($i = 1, \ldots, R$, where R is the number of randomization steps.)
2. – If $i = 1$, let $\mathbf{f}_k^*$ equal to the principal component of $\mathbf{F}_k^*$. Else, calculate the eigenvalue decomposition $\mathbf{F}_k^* = \mathbf{Q}\mathbf{\Lambda}\mathbf{Q}^H$, then the candidate vector is generated as $\mathbf{f}_k^* = \mathbf{Q}\mathbf{\Lambda}^{\frac{1}{2}}\mathbf{w}$, where $\mathbf{w}$ is an i.i.d. complex Gaussian vector with zero mean and unit variance.
   – Solve problem (65) to obtain the optimal $\{\varphi_k^*, \rho_k^*\}$. If the problem turns out to be infeasible, discard that candidate vector. Otherwise, save the candidate $\{\mathbf{f}_k^*, \varphi_k^*, \rho_k^*\}$ and the objective value of the problem.

   End
4. Select the candidate $\{\mathbf{f}_k^*, \varphi_k^*, \rho_k^*\}$ which corresponds to the minimum objective value.

As in our previous work [27], it can be shown that the above optimization problem admits a closed-form solution but we omit the detailed derivation due to space limitation. The proposed rank-one recovery method is summarized in Table VII.[15]

APPENDIX B
THE PROOF OF PROPOSITION 1

Let $P(\mathbf{W}, \{\mathbf{f}_k, \rho_k\}) \triangleq P_B + P_R$ denote the objective function value of problem (13) and n be the iteration number. Clearly, given $\mathbf{W}$, the optimal solution $\{\mathbf{f}_k, \rho_k\}$ can be obtained by solving (15), which results in $P(\mathbf{W}^n, \{\mathbf{f}_k, \rho_k\}^n) \geq P(\mathbf{W}^n, \{\mathbf{f}_k, \rho_k\}^{n+1})$. Similarly, for the given $\{\mathbf{f}_k, \rho_k\}$, we have $P(\mathbf{W}^n, \{\mathbf{f}_k, \rho_k\}^{n+1}) \geq P(\mathbf{W}^{n+1}, \{\mathbf{f}_k, \rho_k\}^{n+1})$.[16] Note that in each iteration of this algorithm, the objective function value is non-increasing and also lower bounded by zero, thus the monotonic convergence of the iterative algorithm in Table I follows.

APPENDIX C
THE PROOF OF PROPOSITION 2

We first introduce four sets of auxiliary variables d_k, $\tilde{d}_k$, e_k and $\tilde{e}_k$, $\forall k \in \mathcal{K}$, which satisfy $d_k = \sigma_r^2 \mathbf{h}_k^H \mathbf{h}_k + \frac{1}{4}\omega_k^2 (p_k^{(i)} - \varphi_l^{(i)})^2 + \frac{1}{\gamma_k}\mathbf{f}_k^{(i)H}\tilde{\mathbf{G}}_k\mathbf{f}_k^{(i)}$, $\tilde{d}_k = -\sigma_k^2\varphi_l + \frac{1}{2}(p_k^{(i)} - \varphi_l^{(i)})(p_k - \varphi_l) + \frac{2}{\gamma_k}\Re\{\mathbf{f}_k^{(i)H}\tilde{\mathbf{G}}_k\mathbf{f}_k\}$, $e_k = -\sigma_r^2\mathbf{h}_k^H\mathbf{h}_k + \sum_{j=1}^{K}\mathbf{f}_j^{(i)H}\tilde{\mathbf{G}}_k\mathbf{f}_j^{(i)} + \frac{\psi_k}{4\xi_k}(q_k^{(i)} - \varphi_l^{(i)})^2$, and $\tilde{e}_k = 2\Re\{\sum_{j=1}^{K}\mathbf{f}_j^{(i)H}\tilde{\mathbf{G}}_k\mathbf{f}_j\} + \frac{\psi_k}{2\xi_k}(q_k^{(i)} - \varphi_l^{(i)})(q_k - \varphi_l) + \sigma_k^2\varphi_l$, where d_k and e_k are constant scalars while $\tilde{d}_k$ and $\tilde{e}_k$ are affine functions in $\mathbf{r}$. Then, the SINR constraints in problem (49) can be rewritten as the following SOCs:

$$\left\| \left[\mathbf{w}_k^T, \frac{\tilde{d}_k - d_k - 1}{2} \right] \right\| \leq \frac{\tilde{d}_k - d_k + 1}{2}, \quad \forall k, \tag{67}$$

where

$$\mathbf{w}_k = [\mathbf{h}_k^H\mathbf{T}_l\mathbf{G}\mathbf{f}_1, \ldots, \mathbf{h}_k^H\mathbf{T}_l\mathbf{G}\mathbf{f}_{k-1}, \mathbf{h}_k^H\mathbf{T}_l\mathbf{G}\mathbf{f}_{k+1}, \ldots, \mathbf{h}_k^H\mathbf{T}_l\mathbf{G}\mathbf{f}_K, \frac{1}{2}\omega_k(p_k + \varphi_l)]^T. \tag{68}$$

Similarly, the EH constraints in problem (49) can be reformulated as the following SOCs:

$$\left\| \left[\sqrt{\frac{\psi_k}{4\xi_k}}(q_k + \varphi_l), \frac{\tilde{e}_k - e_k - 1}{2} \right] \right\| \leq \frac{\tilde{e}_k - e_k + 1}{2}, \quad \forall k. \tag{69}$$

Next, by introducing slack variables P_1, P_2 and P_3, we can equivalently write the objective function $P_l(\mathbf{r})$ of problem (49) as follows:

$$P_l(\mathbf{r}) = P_1 + P_2 + P_3, \tag{70}$$

where

$$\|[\mathbf{f}_1^T, \ldots, \mathbf{f}_K^T, (P_1 - 1)/2]\| \leq (P_1 + 1)/2, \tag{71}$$

$$\|[(\mathbf{G}\mathbf{f}_1)^T, \ldots, (\mathbf{G}\mathbf{f}_K)^T, (P_2 - \varphi_l)/2]\| \leq (P_2 + \varphi_l)/2, \tag{72}$$

$$\|[2\sigma_r, \varphi_l - P_3]\| \leq \varphi_l + P_3. \tag{73}$$

Therefore, problem (49) can be shown to be equivalent to (50).

[15] We only list the detailed steps to recover $\mathbf{f}_k^*$, which can be easily extended to the recovery of $\mathbf{W}^*$.

[16] Due to the Gaussian randomization procedure employed in the recovery method, the total transmission power of Step 2.2 could be possibly larger than that of Step 2.1. When this happens, we simply terminate the algorithm and achieve convergence in a finite number of iterations, as indicated in Step 3.

REFERENCES

[1] L. R. Varshney, "Transporting information and energy simultaneously," in *Proc. IEEE Int. Symp. Inf. Theory (ISIT)*, Jul. 2008, pp. 1612–1616.
[2] P. Grover and A. Sahai, "Shannon meets Tesla: Wireless information and power transfer," in *Proc. IEEE Int. Symp. Inf. Theory (ISIT)*, Jun. 2010, pp. 2363–2367.
[3] P. Popovski and O. Simeone, "Two-way communication with energy exchange," in *Proc. IEEE Inf. Theory Workshop*, Sep. 2012, pp. 592–596.
[4] A. M. Fouladgar and O. Simeone, "On the transfer of information and energy in multi-user systems," *IEEE Commun. Lett.*, vol. 16, no. 11, pp. 1733–1736, Nov. 2012.
[5] R. Zhang and C. K. Ho, "MIMO broadcasting for simultaneous wireless information and power transfer," *IEEE Trans. Wireless Commun.*, vol. 12, no. 5, pp. 1989–2001, May 2013.
[6] L. Liu, R. Zhang, and K.-C. Chua, "Wireless information and power transfer: A dynamic power splitting approach," *IEEE Trans. Commun.*, vol. 61, no. 9, pp. 3990–4001, Sep. 2013.
[7] X. Zhou, R. Zhang, and C. K. Ho, "Wireless information and power transfer: Architecture design and rate-energy tradeoff," *IEEE Trans. Commun.*, vol. 61, no. 11, pp. 4754–4767, Nov. 2013.
[8] Q. Shi, W. Xu, L. Liu, and R. Zhang, "Joint transmit beamforming and receive power splitting for MISO SWIPT systems," *IEEE Trans. Wireless Commun.*, vol. 13, no. 6, pp. 3269–3280, Jun. 2014.
[9] S. Timotheou, I. Krikidis, G. Zheng, and B. Ottersten, "Beamforming for MISO interference channels with QoS and RF energy transfer," *IEEE Trans. Wireless Commun.*, vol. 13, no. 5, pp. 2646–2658, May 2014.
[10] Q. Shi, W. Xu, T. H. Chang, Y. Wang, and E. Song, "Joint beamforming and power splitting for MISO interference channel with SWIPT: An SOCP relaxation and decentralized algorithm," *IEEE Trans. Signal Process.*, vol. 62, no. 23, pp. 6194–6208, Dec. 2014.
[11] B. K. Chalise, Y. D. Zhang, and M. G. Amin, "Energy harvesting in an OSTBC based amplify-and-forward MIMO relay system," in *Proc. IEEE Int. Conf. Acoust., Speech Signal Process.*, Mar. 2012, pp. 3201–3204.
[12] Q. Li, Q. Zhang, and J. Qin, "Beamforming in non-regenerative two-way multi-antenna relay networks for simultaneous wireless information and power transfer," *IEEE Trans. Wireless Commun.*, vol. 13, no. 10, pp. 5509–5520, Oct. 2014.
[13] G. Li, P. Ren, G. Lv, and Q. Du, "High-rate relay beamforming for simultaneous wireless information and power transfer," *Electron. Lett.*, vol. 50, no. 23, pp. 1759–1761, 2014.
[14] H. Chen, Y. Li, Y. Jiang, Y. Ma, and B. Vucetic, "Distributed power splitting for SWIPT in relay interference channels using game theory," *IEEE Trans. Wireless Commun.*, vol. 14, no. 1, pp. 410–420, Jan. 2015.

[15] T. Tang, C.-B. Chae, R. W. Heath, and S. Cho, "On achievable sum rates of a multiuser MIMO relay channel," in *Proc. IEEE Int. Symp. Inf. Theory (ISIT)*, Jul. 2006, pp. 1026–1030.

[16] K. S. Gomadam and S. A. Jafar, "On the duality of MIMO MAC and BC with AF relays," in *Proc. IEEE Asilomar Conf. Signals, Syst. Comput.*, Nov. 2007, pp. 863–867.

[17] R. Zhang, C. C. Chai, and Y.-C. Liang, "Joint beamforming and power control for multiantenna relay broadcast channel with QoS constraints," *IEEE Trans. Signal Process.*, vol. 57, no. 2, pp. 726–737, Feb. 2009.

[18] D. Feng, C. Jiang, G. Lim, L. J. Cimini, Jr., G. Feng, and G. Y. Li, "A survey of energy-efficient wireless communications," *IEEE Commun. Surveys Tut.*, vol. 15, no. 1, pp. 167–178, 1st Quart., 2013.

[19] G. Y. Li *et al.*, "Energy-efficient wireless communications: Tutorial, survey, and open issues," *IEEE Wireless Commun.*, vol. 18, no. 6, pp. 28–35, Dec. 2011.

[20] N. Banerjee, M. D. Corner, D. Towsley, and B. N. Levine, "Relays, base stations, and meshes: Enhancing mobile networks with infrastructure," in *Proc. MobiCom*, San Francisco, CA, USA, Sep. 2008, pp. 81–91.

[21] Z.-Q. Luo, W.-K. Ma, A. M.-C. So, Y. Ye, and S. Zhang, "Semidefinite relaxation of quadratic optimization problems," *IEEE Signal Process. Mag.*, vol. 27, no. 3, pp. 20–34, May 2010.

[22] S. Boyd and L. Vandenberghe, *Convex Optimization*. Cambridge, U.K.: Cambridge Univ. Press, 2004.

[23] S. Boyd, L. El Ghaoui, E. Feron, and V. Balakrishnan, *Linear Matrix Inequalities in System and Control Theory*, vol. 15. Philadelphia, PA, USA: SIAM, 1994.

[24] Y. Cai, R. C. D. Lamare, L.-L. Yang, and M. Zhao, "Robust MMSE precoding based on switched relaying and side information for multiuser MIMO relay systems," *IEEE Trans. Veh. Technol.*, vol. 64, no. 12, pp. 5677–5687, Dec. 2015.

[25] A. L. Yuille and A. Rangarajan, "The concave-convex procedure," *Neural Comput.*, vol. 15, no. 4, pp. 915–936, 2003.

[26] G. R. Lanckriet and B. K. Sriperumbudur, "On the convergence of the concave-convex procedure," in *Proc. Adv. Neural Inf. Process. Syst.*, 2009, pp. 1759–1767.

[27] M.-M. Zhao, Y. Cai, Q. Shi, B. Champagne, and M.-J. Zhao, "Robust transceiver design for MISO interference channel with energy harvesting," *IEEE Trans. Signal Process.*, vol. 64, no. 17, pp. 4618–4633, Sep. 2016.

[28] J. N. Laneman, G. W. Wornell, and D. N. C. Tse, "An efficient protocol for realizing cooperative diversity in wireless networks," in *Proc. IEEE Int. Symp. Inf. Theory (ISIT)*, Jun. 2001, p. 294.

[29] X. Lu, P. Wang, D. Niyato, D. I. Kim, and Z. Han, "Wireless networks with RF energy harvesting: A contemporary survey," *IEEE Commun. Surveys Tut.*, vol. 17, no. 2, pp. 757–789, 2nd Quart., 2015.

[30] T. Kong and Y. Hua, "Optimal design of source and relay pilots for MIMO relay channel estimation," *IEEE Trans. Signal Process.*, vol. 59, no. 9, pp. 4438–4446, Sep. 2011.

[31] S. Sun and Y. Jing, "Channel training design in amplify-and-forward MIMO relay networks," *IEEE Trans. Wireless Commun.*, vol. 10, no. 10, pp. 3380–3391, Oct. 2011.

[32] F.-S. Tseng, W.-J. Huang, and W.-R. Wu, "Robust far-end channel estimation in three-node amplify-and-forward MIMO relay systems," *IEEE Trans. Veh. Technol.*, vol. 62, no. 8, pp. 3752–3766, Oct. 2013.

[33] F. W. Vook, X. Zhuang, K. L. Baum, and T. A. Thomas, *Signaling Methodologies to Support Closed-Loop Transmit Processing in TDD-OFDMA*, IEEE Standard C802.16e-04/103r2, Jul. 2004.

[34] S. A. Vorobyov, A. B. Gershman, and Z.-Q. Luo, "Robust adaptive beamforming using worst-case performance optimization: A solution to the signal mismatch problem," *IEEE Trans. Signal Process.*, vol. 51, no. 2, pp. 313–324, Feb. 2003.

[35] M. Biguesh, S. Shahbazpanahi, and A. B. Gershman, "Robust downlink power control in wireless cellular systems," *EURASIP J. Wireless Commun. Netw.*, vol. 2, pp. 261–272, Jul. 2004.

[36] M. Payaro, A. Pascual-Iserte, and M. A. Lagunas, "Robust power allocation designs for multiuser and multiantenna downlink communication systems through convex optimization," *IEEE J. Sel. Areas Commun.*, vol. 25, no. 7, pp. 1390–1401, Sep. 2007.

[37] G. Caire, N. Jindal, M. Kobayashi, and N. Ravindran, "Multiuser MIMO achievable rates with downlink training and channel state feedback," *IEEE Trans. Inf. Theory*, vol. 56, no. 6, pp. 2845–2866, Jun. 2010.

[38] J. Xu, L. Liu, and R. Zhang, "Multiuser MISO beamforming for simultaneous wireless information and power transfer," *IEEE Trans. Signal Process.*, vol. 62, no. 18, pp. 4798–4810, Sep. 2014.

[39] S. Lee, L. Liu, and R. Zhang, "Collaborative wireless energy and information transfer in interference channel," *IEEE Trans. Wireless Commun.*, vol. 14, no. 1, pp. 545–557, Jan. 2015.

[40] R. H. Tütüncü, K. C. Toh, and M. J. Todd, "Solving semidefinite-quadratic-linear programs using SDPT3," *Math. Program.*, vol. 95, no. 2, pp. 189–217, 2003.

[41] U. Rashid, H. D. Tuan, and H. H. Nguyen, "Relay beamforming designs in multi-user wireless relay networks based on throughput maximin optimization," *IEEE Trans. Commun.*, vol. 61, no. 5, pp. 1739–1749, May 2013.

[42] Y. Cheng and M. Pesavento, "Joint optimization of source power allocation and distributed relay beamforming in multiuser peer-to-peer relay networks," *IEEE Trans. Signal Process.*, vol. 60, no. 6, pp. 2962–2973, Jun. 2012.

[43] D. H. Brandwood, "A complex gradient operator and its application in adaptive array theory," *IEE Proc. F Commun., Radar Signal Process.*, vol. 130, no. 1, pp. 11–16, Feb. 1983.

[44] G. Zheng, S. Chatzinotas, and B. Ottersten, "Generic optimization of linear precoding in multibeam satellite systems," *IEEE Trans. Wireless Commun.*, vol. 11, no. 6, pp. 2308–2320, Jun. 2012.

[45] H. Pennanen, A. Tölli, and M. Latva-Aho, "Decentralized robust beamforming for coordinated multi-Cell MISO networks," *IEEE Signal Process. Lett.*, vol. 21, no. 3, pp. 334–338, Mar. 2014.

[46] K.-Y. Wang, A. M.-C. So, T.-H. Chang, W.-K. Ma, and C.-Y. Chi, "Outage constrained robust transmit optimization for multiuser MISO downlinks: Tractable approximations by conic optimization," *IEEE Trans. Signal Process.*, vol. 62, no. 21, pp. 5690–5705, Nov. 2014.

[47] Y. Zeng and R. Zhang, "Full-duplex wireless-powered relay with self-energy recycling," *IEEE Wireless Commun. Lett.*, vol. 4, no. 2, pp. 201–204, Apr. 2015.

[48] J. Xu and R. Zhang, "A general design framework for MIMO wireless energy transfer with limited feedback," *IEEE Trans. Signal Process.*, vol. 64, no. 10, pp. 2475–2488, May 2016.

[49] C. R. Inc. (Sep. 2012). *CVX: MATLAB Software for Disciplined Convex Programming*. [Online]. Available: http://cvxr.com/cvx

[50] J. Li, P. Stoica, and Z. Wang, "On robust Capon beamforming and diagonal loading," *IEEE Trans. Signal Process.*, vol. 51, no. 7, pp. 1702–1715, Jul. 2003.

[51] J. Li, P. Stoica, and Z. Wang, "Doubly constrained robust Capon beamformer," *IEEE Trans. Signal Process.*, vol. 52, no. 9, pp. 2407–2423, Sep. 2004.

[52] S.-J. Kim, A. Magnani, A. Mutapcic, S. P. Boyd, and Z.-Q. Luo, "Robust beamforming via worst-case SINR maximization," *IEEE Trans. Signal Process.*, vol. 56, no. 4, pp. 1539–1547, Apr. 2008.

Yunlong Cai (S'07–M'10–SM'16) received the B.S. degree in computer science from Beijing Jiaotong University, Beijing, China, in 2004, the M.Sc. degree in electronic engineering from the University of Surrey, Guildford, U.K., in 2006, and the Ph.D. degree in electronic engineering from the University of York, York, U.K., in 2010. From 2010 to 2011, he was a Post-Doctoral Fellow with the Electronics and Communications Laboratory, Conservatoire National des Arts et Metiers, Paris, France. Since 2011, he has been with the Department of Information Science and Electronic Engineering, Zhejiang University, Hangzhou, China, where he is currently an Associate Professor. His research interests include spread spectrum communications, adaptive signal processing, multiuser detection, and multiple antenna systems.

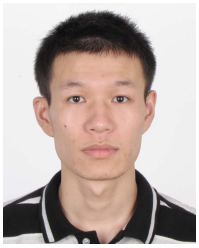

Ming-Min Zhao received the B.S. degree in information and communication engineering from Zhejiang University, Hangzhou, China, in 2012. He is currently pursuing the Ph.D. degree with the College of Information Science and Electronic Engineering, Zhejiang University. His research interests include algorithm design and analysis for MIMO communication systems, cooperative communications, and energy harvesting.

Qingjiang Shi received the Ph.D. degree in communication engineering from Shanghai Jiao Tong University, Shanghai, China, in 2011. From 2009 to 2010, he visited Prof. Z.-Q. (Tom) Luo Research Group with the University of Minnesota, Twin Cities. In 2011, he was a Research Scientist with the Research and Innovation Center (Bell Labs China), Alcatel-Lucent, Shanghai. He is currently an Associate Professor with the School of Information and Science Technology, Zhejiang Sci-Tech University, Hangzhou, China. His current research interests lie in algorithm design for signal processing in advanced MIMO, cooperative communication, physical layer security, energy-efficient communication, wireless information and power transfer.

Dr. Shi received the National Excellent Doctoral Dissertation Nomination Award in 2013, the Shanghai Excellent Doctoral Dissertation Award in 2012, and the best paper award from the IEEE PIMRC'09 Conference.

Benoit Champagne (S'87–M'89–SM'03) received the B.Eng. degree in engineering physics from the École Polytechnique de Montréal in 1983, the M.Sc. degree in physics from the Université de Montréal in 1985, and the Ph.D. degree in electrical engineering from the University of Toronto in 1990. From 1990 to 1999, he was an Assistant and then an Associate Professor with INRS-Telecommunications, Université du Quebec, Montréal. In 1999, he joined McGill University, Montréal, where he is currently a Full Professor with the Department of Electrical and Computer Engineering. He also served as an Associate Chairman of the Graduate Studies with the Department from 2004 to 2007. His research focuses on the study of advanced algorithms for the processing of communication signals by digital means. His interests span many areas of statistical signal processing, including detection and estimation, sensor array processing, adaptive filtering, and applications thereof to broadband communications and audio processing, where he has co-authored nearly 250 referred publications. His research has been funded by the Natural Sciences and Engineering Research Council of Canada, the Fonds de Recherche sur la Nature et les Technologies from the Government of Quebec, and some major industrial sponsors, including Nortel Networks, Bell Canada, InterDigital and Microsemi.

Dr. Champagne has been an Associate Editor of the *EURASIP Journal on Advances in Signal Processing* from 2005 to 2007, the IEEE SIGNAL PROCESSING LETTERS from 2006 to 2008, and the IEEE TRANSACTIONS ON SIGNAL PROCESSING from 2010 to 2012, and a Guest Editor of two special issues of the *EURASIP Journal on Advances in Signal Processing* published in 2007 and 2014, respectively. He has also served on the Technical Committees of several international conferences in communications and signal processing. He was a Registration Chair of the IEEE ICASSP 2004, the Co-Chair, Antenna and Propagation Track, of the IEEE VTC-Fall 2004, the Co-Chair, Wide Area Cellular Communications Track, of the IEEE PIMRC 2011, the Co-Chair, Workshop on D2D Communications, of the IEEE ICC 2015 and the Publicity Chair of the IEEE VTC-Fall 2016.

Min-Jian Zhao (M'10) received the M.Sc. and Ph.D. degrees in communication and information systems from Zhejiang University, Hangzhou, China, in 2000 and 2003, respectively.

He is currently a Professor with the Department of Information Science and Electronic Engineering, Zhejiang University. His research interests include modulation theory, channel estimation and equalization, and signal processing for wireless communications.